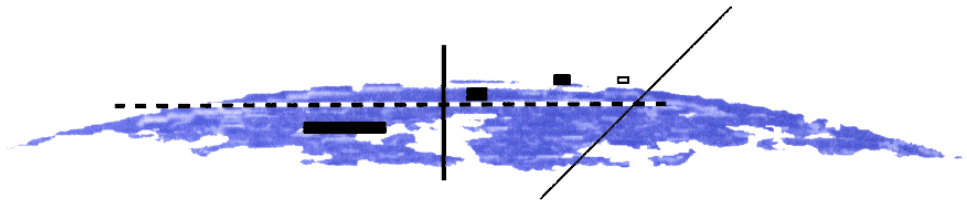

GeoForschungsZentrum Potsdam
STIFTUNG DES ÖFFENTLICHEN RECHTS

Alexander N. Marchenko
Franz Barthelmes
Uwe Meyer
Peter Schwintzer

Regional Geoid Determination: An Application to Airborne Gravity Data in the Skagerrak

Scientific Technical Report STR01/07

Imprint

GeoForschungsZentrum Potsdam

Telegrafenberg
D-14473 Potsdam
e-mail: postmaster@gfz-potsdam.de
www: http://www.gfz-potsdam.de

Printed in Potsdam, Germany
June 2001

Alexander N. Marchenko
Franz Barthelmes
Uwe Meyer
Peter Schwintzer

Regional Geoid Determination: An Application to Airborne Gravity Data in the Skagerrak

Scientific Technical Report STR01/07

REGIONAL GEOID DETERMINATION: AN APPLICATION TO AIRBORNE GRAVITY DATA IN THE SKAGERRAK

A.N. Marchenko[1,2], F. Barthelmes[1], U. Meyer[1], P. Schwintzer[1]

[1]GeoForschungsZentrum Potsdam (GFZ),
Division "Kinematics and Dynamics of the Earth"
D-14473 Potsdam, Telegrafenberg A17, Germany
march@gfz-potsdam.de, bar@gfz-potsdam.de,
umeyer@gfz-potsdam.de, psch@gfz-potsdam.de

[2]National University "Lviv Polytechnic",
S. Bandera St. 12, UA-79013 Lviv, Ukraine
march@polynet.lviv.ua

Summary: Regarding the rapidly growing airborne gravimetric data base worldwide, an investigation to study efficient and stable geoid computations based on this type of data was assessed to be important. The presented study comprehends different approaches to compute a regional geoid from existing airborne gravimetry data and its combination with further available data sets. The efficiency and quality of results for the different approaches and data combinations are discussed.

The data sets used are: 1) Airborne gravimetry in the Skagerrak acquired during the AGMASCO EU-project (MAS3-CT95-0014), 2) Marine gravity data in the Skagerrak extracted from the BGI data base, 3) UEGN94 absolute gravimetric network data.

The methods applied on this data sets are: 1) collocation, 2) collocation with regularization, 3) approximation by radial multipole potentials, including point mass potentials.

For collocation and collocation with regularization kernel functions corresponding to radial multipoles are used.

The concluding results of the investigation are: 1) collocation with regularization provides more accurate results than the standard collocation method using the same reproducing kernel, 2) higher stability of solutions is achieved by including absolute gravimetric network data, 3) the approximation by radial multipole potentials is recommended especially for fast computations of the geoid from airborne data without loss of accuracy.

Comparisons of all solutions worked out in this study with the geoid model for the European nordic countries show a good agreement (mean deviation < 0.5 cm; rms < 5 cm). This noise level corresponds to an estimated geoid accuracy of better than 10 cm for the Skagerrak.

Key words: Airborne geoid – Collocation – Regularization – Reproducing kernels – Radial multipoles

Contents

1 Introduction

The geoid determination has recently reached a new level of development. With modern satellite techniques at hand as *altimetry* and *GPS*, the geoid becomes "directly observable". Thus, we can "measure" it on any given set of points: over oceans by means of satellite altimetry in combination with an ocean circulation model, over continents with the help of GPS positioning and precise leveling (GPS-leveling). The latest progress of geoid determination is connected with up-to-date developments in airborne and space techniques and requires appropriate mathematical methods to combine the different types of data with the highest possible accuracy. The intention of this paper is to construct a regional geoid on the basis of airborne data using different mathematical approximation methods. In particular, we will apply and investigate variations of the collocation method developed in physical geodesy. The *remove-restore technique* is used to get rid of the low frequency gravity field content.

The traditional gravimetric geoid determination is based on *gravity anomalies* Δg which are given (by leveling) with respect to the geoid (which is unknown at this stage and has to be determined using just these gravity measurements). With the modern GPS technique today, the position of the gravity measurements (especially the airborne) are known with respect to an Earth-fixed coordinate system and the geodetic functional connected to this problem is the *gravity disturbance* δg (for definition of Δg and δg c.f. Heiskanen and Moritz, 1967). Nevertheless, in this study we prefer gravity anomalies, as traditionally used in geodesy, rather than gravity disturbances because of their better compatibility with already existing measurements over land and sea.

The airborne gravimetric data set used for this study was acquired in 1996 within the scope of the EU-project *AGMASCO* (Airborne Geoid Mapping System for Coastal Oceanography, EU-MAST project MAS3-CT95-0014). The main instruments used were a LaCoste&Romberg ship and air gravimeter type S99 of the University Bergen on board a Dornier-228 aircraft of the Alfred-Wegener-Institute for Polar and Marine Research, Bremerhaven, plus several airborne and land based Trimble 4000 GPS receivers. A detailed project description is found in Forsberg et al. (1997). The data set was chosen because of the high quality of the airborne data set (root mean square (rms) less than 2.5 mGal), its homogeneous distribution (15 km line spacing, 1 Hz sampling, 6 km spatial resolution, 400 m mean altitude), the regional extent of the area (150 km $\times$ 250 km) and good ground control on the coastlines by GPS reference stations and gravimetric networks. Thus, an appropriate subset of the UEGN94 network of absolute gravimetry (Boedecker et al., 1995) was additionally used.

2 Remove-restore technique for geoid determination

In practice, the solution of the central problem in physical geodesy results in determining an equipotential surface W of the Earth's gravity field in a body-fixed coordinate

system. The fundamental equipotential surface, the geoid, is defined by

$$W(x, y, z) = W_0 = const \quad . \tag{1}$$

W_0 is chosen such that the geoid surface is close to the mean sea surface. (The reader should distinguish the concept of the *"geoid"* from the concept of the *"quasi-geoid"* which are connected in practice with the application of *"orthometric heights"* H or *"normal heights"* H^γ respectively. The quasi-geoid is the surface obtained by subtracting the normal height from the elevation of the surface points, and is no equipotential surface.) The geoid computation requires the solution of Eq. (1). As a

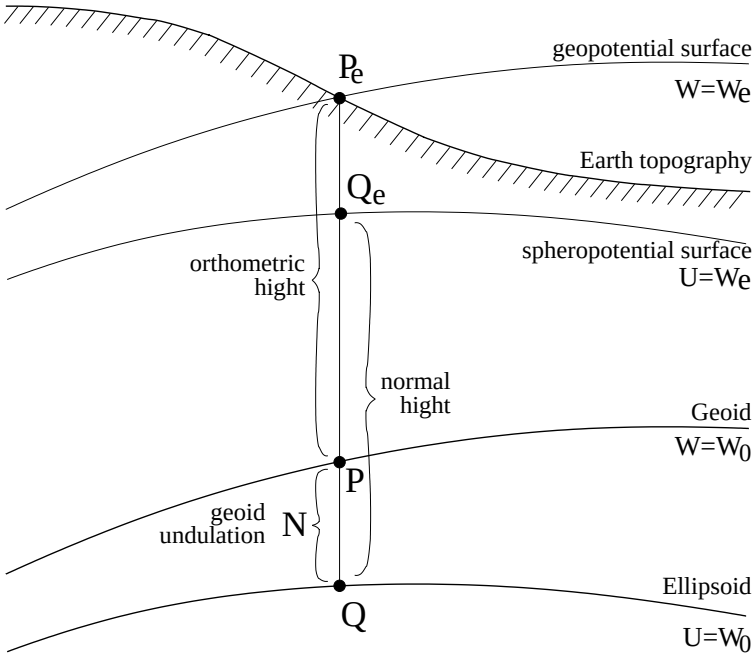

Figure 1: The basic geometry

result, if we compare the gravity potential $W = W_0$ at the point P on the geoid (see Fig. 1)

$$W(P) = U(P) + T(P) = const = W_0 \quad , \tag{2}$$

with the normal potential $U = U_0$ of the reference ellipsoid at the point Q

$$U(Q) = U_0 = W(P) = W_0 = const \quad , \tag{3}$$

we define the anomalous potential T as the difference between W_0 and the potential $U(P)$ of the reference ellipsoid at point P. The corresponding geoid undulation N is found by means of the Bruns formula

$$N = \frac{T}{\gamma} \quad , \tag{4}$$

in combination with the definition of the gravity anomaly (by introducing the normal gravity γ):

$$\Delta g = g(P) - \gamma(Q) = g_P - \gamma_Q \quad . \tag{5}$$

This results in the fundamental equation of physical geodesy:

$$\frac{\partial T}{\partial h} - \frac{1}{\gamma}\frac{\partial \gamma}{\partial h} T = -\Delta g = -(g_P - \gamma_Q) \quad . \tag{6}$$

If Δg is known it is possible to solve the boundary value problem to find T and the geoid undulation N (gravimetric geoid) above the reference ellipsoid.

Regional and local geoid computations usually are carried out using the *remove-restore technique* where parts of the gravity field well known from other measurements are subtracted (removed) before data approximation and are then added again (restored) afterwards. Generally, these are the long wavelengths part, known from global satellite based geopotential models and the short wavelengths part known from topography. In other words the geoid height N is composed of (Forsberg and Tscherning, 1981)

$$N = N_M + N_T + N_R \quad , \tag{7}$$

where N_M, N_T, N_R are the contributions of the global geopotential model, the terrain effect of the topographic masses, and the residual geoid, respectively. Now the residual geoid can be modeled from the gravity observations. According to Eq. (7) the gravity anomaly Δg is split up into the same contributions

$$\Delta g = \Delta g_M + \Delta g_T + \Delta g_R \quad . \tag{8}$$

Because the quantities Δg_M and Δg_T can be computed by means of suitable models, these effects are *"removed"* from the gravity anomaly

$$\Delta g_R = \Delta g - (\Delta g_M + \Delta g_T) \quad , \tag{9}$$

to give the initial information Δg_R for the determination of N_R. Thus, the next step will be a straightforward application of one of the known mathematical methods to approximate the geoid undulations N_R using these new "observations" Δg_R. In the sequel the constituents N_M and N_T are restored to yield the complete geoid hight N.

If the gravimetric geoid for the whole Earth is determined by least-squares collocation (Moritz, 1980) or by the variational method of physical geodesy (Neyman, 1979) the following basic requirement must be met:

$$\frac{1}{4\pi} \iint_{\sigma} \Delta g \, d\sigma = M\{\Delta g\} = 0 \quad . \tag{10}$$

That means the spherical harmonic expression of the potential T and the gravity anomalies Δg must not contain terms of degree zero. The symbol M in Eq. (10) denotes the average over the spherical Earth with the surface σ. Furthermore

$$M\{T\} = 0 \quad , \tag{11}$$

must hold for the anomalous potential T. Generally these requirements (Eqs. 10 and 11) are not fulfilled a priori, therefore in case of regional or local geoid determination "centered measurements" Δg^* are computed after having removed the contribution of a global gravity model of high resolution. It is assumed that the influence of the distant zones can be neglected. This requirement is fulfilled to a better approximation with increasing accuracy and resolution of the removed global model.

The recent progress in determining high resolution global gravity field models has been documented e.g. in Lemoine et al. (1998) and Gruber (2000). The highest resolution of these models is up to terms of degree $l_{\max} = 360$, corresponding to a spatial resolution of $\lambda/2 = 30'$ (half wavelength) according to

$$\frac{\lambda}{2} = \frac{180^\circ}{l_{\max}} \quad . \tag{12}$$

In this paper we will use only gravity as input data. Therefore, we can determine the gravimetric geoid only, which usually is characterized by a high resolution with high relative accuracy but only moderate absolute accuracy. One of the explanations for the latter is an insufficient accuracy of W_0 (see Eq. 1). The combination with GPS-leveling derived geoid heights could overcome this problem and would lead to an absolute frame. Nevertheless, our main goal is to derive a regional relative geoid model using gravity anomalies and the remove-restore technique. As the mathematical method for approximating the geoid we try different modifications of the collocation method.

3 General remarks on the linearization of geodetic functionals

Next, according to Moritz (1980) we will start from the general view that each measurement ℓ is a nonlinear functional which depends on the Earth's gravity field, on one or several points in space and on time t:

$$\ell = F[\mathbf{X}\,(t)\,, W\,(t)] \quad . \tag{13}$$

Here $W(t)$ denotes the *time-dependent* gravity potential of the Earth that may be represented as the sum of the time-dependent gravitational potential $V(t)$ and the potential $\Phi(t)$ of the centrifugal force

$$W(t) = V(t) + \Phi(t), \quad \text{(in practice:} \quad \Phi(t) = const). \tag{14}$$

The time-dependent vector $\mathbf{X}(t)$ consists of the time-dependent coordinates of the point, where a measurement was made. If we shall assume $t = const$, from Eqs. (13) and (14) we get

$$\ell = F\left[\mathbf{X}\,(t = const)\,, W\,(t = const)\right] = F\left[\mathbf{X}, \mathbf{W}\right], \quad t = const, \tag{15}$$

$$W(t = const) = V(t = const) + \Phi(t = const) = W = V + \Phi, \quad t = const, \qquad (16)$$

that will not differ from those in Moritz (1980) if the corresponding *correction to a convenient reference epoch is presupposed.* Hence, we can formally work for each $t = const$ with *time-independent* vector $\mathbf{X}$ and potential W. So, denoting the number of components of the vector $\mathbf{X}$ by p ($\mathbf{X}$ is an element of the p-dimensional Euclidean space $\mathbf{R}^p$) we get

$$\ell = F[\mathbf{X}, V + \Phi] \quad , \qquad (17)$$

or

$$\ell = F[\mathbf{X}, W] \quad . \qquad (18)$$

The function V belongs to some Hilbert space H of harmonic functions; for every fixed t the functional F is a mapping of the product space $\mathbf{R}^p \times H$ into the set $\mathbf{R}$ of real numbers. For different kinds of measurements we shall obtain different functionals F, which in the general case are nonlinear ones. Due to the fact that the potential V belongs to the infinite dimensional space H and the number of measurements or functionals of V are always finite, the inverse geodetic problem does not have a unique solution. In other words, the determination of the Earth's gravity field is an *"improperly posed"* or *"ill-posed"* problem.

Obviously, it will be complicated in practice to use Eq. (18) directly. The traditional way to solve nonlinear problems consists of their linearization by Taylor's theorem and the direct solution of the linear problem. Thus, the solution of a nonlinear problem splits into two steps: *linearization* and *solution* of the system of linear equations.

The linearization of nonlinear functionals can be provided (Moritz, 1980) by introducing the approximations $\mathbf{X}_0$ for the vector $\mathbf{X}$ and U for the gravity potential W:

$$\mathbf{X} = \mathbf{X}_0 + \delta\mathbf{X} \quad , \qquad (19)$$

$$W = U + T \quad , \qquad (20)$$

$$\delta\mathbf{X} = \mathbf{X} - \mathbf{X}_0 \quad , \qquad (21)$$

$$T = W - U \quad , \qquad (22)$$

where U is the normal gravity potential (e.g. of an ellipsoid of revolution); the differences in Eqs. (21) and (22) are considered to be small; T is the anomalous potential. It can be derived from Eqs. (18), (19) and (20) that the following expression is valid

$$\ell = F\left[\mathbf{X}_0 + \delta\mathbf{X}, U + T\right] \quad . \qquad (23)$$

Taylor's expansion of Eq. (23) gives

$$\ell = F\left[\mathbf{X}_0, U\right] + \mathbf{a}^T \delta\mathbf{X} + LT \quad , \tag{24}$$

neglecting the second and higher order terms. Here $\mathbf{a}$ is the column vector that consists of the ordinary partial derivatives a_k of $F[\mathbf{X}, W]$ with respect to the components X_k of the vector $\mathbf{X}$; the approximate values $\mathbf{X}_0$ and U are taken instead of the unknown values $\mathbf{X}$ and W:

$$a_k = \left.\frac{\partial F[\mathbf{X}, W]}{\partial X_k}\right|_{\mathbf{X}_0, U} \quad . \tag{25}$$

The term $\mathbf{a}^T\delta\mathbf{X}$ is the scalar product and LT expresses the linear operator L acting on the disturbing potential T (see, e.g., Eqs. (4) and (6)). Then we note that the simple difference

$$\delta\ell = F\left[\mathbf{X}, W\right] - F\left[\mathbf{X}_0, U\right] \quad , \tag{26}$$

represents the result of linearization: $F\left[\mathbf{X}, W\right]$ is the observation; $F[\mathbf{X}_0, U]$ is the approximate value of $F[\mathbf{X}, W]$ computed with the initial values known a priori. The quantity $\delta\ell$ is called *"observed minus computed"* and contains the information to determine the unknowns δX and T. Let q denote the number of observations. The linearized system may be written now as

$$\left.\begin{array}{l} \delta\ell_1 = \mathbf{a}_1^T\delta\mathbf{X} + L_1T \\ \delta\ell_2 = \mathbf{a}_2^T\delta\mathbf{X} + L_2T \\ \cdots\cdots\cdots\cdots\cdots \\ \delta\ell_q = \mathbf{a}_q^T\delta\mathbf{X} + L_qT \end{array}\right\} \quad . \tag{27}$$

In general, the normal potential U may be more complex than the potential of an ellipsoid but the traditional old denotation U is kept. It is recommendable to use a normal potential U as near as possible to W to minimize the linearization error.

4 Collocation, variational problem and conditions of solvability

For simplicity, we rewrite the system of Eq. (27), which was found by linearization, in the matrix form

$$\boldsymbol{\ell} = \mathbf{A}\mathbf{X} + \mathbf{B}T + \mathbf{n} \quad . \tag{28}$$

Here $\mathbf{X}$ is the p-vector consisting of the components X_i and $\boldsymbol{\ell}$ is the q-vector consisting of the components ℓ_i (changing notation from δX_i to X_i and $\delta\ell_i$ to ℓ_i, resp., in Eq. (27)). The matrix $\mathbf{A}$ of partial derivatives has the dimension $(q \times p)$ and $\mathbf{B}$ is the linear operator, which can be formed from q linear functionals L_i. Thus, we put

$$\boldsymbol{\ell} = \begin{bmatrix} \ell_1 \\ \ell_2 \\ \ldots \\ \ell_q \end{bmatrix}, \quad \mathbf{A} = \begin{bmatrix} \mathbf{a}_1^T \\ \mathbf{a}_2^T \\ \ldots. \\ \mathbf{a}_q^T \end{bmatrix}, \quad \mathbf{B} = \begin{bmatrix} L_1 \\ L_2 \\ \ldots. \\ L_q \end{bmatrix} \quad , \tag{29}$$

assuming that $\mathbf{A}$ has a full rank and $p < q$. The q-vector $\mathbf{n}$ reflects the influence of measurement errors ("noise"); the vector $\mathbf{X}$ and the disturbing potential T in Eq. (28) is going to be determined from the measurements $\boldsymbol{\ell}$.

Let $\mathbf{B}$=0, then Eq. (28) becomes

$$\boldsymbol{\ell} = \mathbf{AX} + \mathbf{n} \quad , \tag{30}$$

that is the system of linear equations in the traditional least-squares adjustment by parameters. The model described by Eq. (28) may be treated as an extension of the standard model of Eq. (30). The terms in Eq. (28) can be considered to belong to the q-dimensional Euclidean space $\mathbf{R}^q$ except $\mathbf{B}T$, which includes the potential T treated as an element of the infinite Hilbert space.

Now we turn to the solution of Eq. (30). We remember that an inverse problem is called *properly posed* (according to *Hadamar*) if its solution satisfies the following requirements:

existence,
uniqueness,
stability.

Generally Eq. (30) does not have an exact solution but under the condition

$$(\boldsymbol{\ell} - \mathbf{AX})^T (\boldsymbol{\ell} - \mathbf{AX}) = \mathbf{n}^T\mathbf{n} = \min \quad , \tag{31}$$

a unique "least squares" estimate of the following form

$$\hat{\mathbf{X}} = \left(\mathbf{A}^T\mathbf{A}\right)^{-1} \mathbf{A}^T\boldsymbol{\ell} \quad , \tag{32}$$

is possible to find if the matrix $\mathbf{A}$ has full rank and $p < q$. Eq. (32) is the solution of the *normal equation* system. Thus the first two conditions for a *properly posed problem* are satisfied by Eq. (32). The third requirement, stability, means that small changes of the observations $\boldsymbol{\ell}$ will only cause small changes of the estimation $\hat{\mathbf{X}}$; i.e. the solution $\hat{\mathbf{X}}$ must be a continuous function of the vector $\boldsymbol{\ell}$. The third requirement may be violated in Eq. (32), then the corresponding problem transforms to an *improperly posed (or ill-posed) problem* (Tikhonov and Arsenin, 1974). There are many examples in which the construction of normal solutions leads to unstable results. A generalization of Eq. (32) is the solution (weighted least-squares adjustment)

$$\hat{\mathbf{X}} = \left(\mathbf{A}^T\mathbf{C}_{\mathbf{nn}}^{-1}\mathbf{A}\right)^{-1} \mathbf{A}^T\mathbf{C}_{\mathbf{nn}}^{-1}\boldsymbol{\ell} \quad , \tag{33}$$

which is obtained *also under the least squares principle*

$$\mathbf{n}^T\mathbf{C}_{\mathbf{nn}}^{-1}\mathbf{n} = \min \quad , \tag{34}$$

with $\mathbf{C}_{\mathrm{nn}}$ being the $(q \times q)$- covariance matrix of measurement noise.

For further use, we return to discuss a solution of Eq. (28) which may be represented in the following form

$$\hat{\mathbf{X}} = \left[\mathbf{A}^T \left(\mathbf{C} + \alpha \mathbf{C}_{\mathbf{nn}}\right)^{-1} \mathbf{A}\right]^{-1} \mathbf{A}^T \left(\mathbf{C} + \alpha \mathbf{C}_{\mathbf{nn}}\right)^{-1} \boldsymbol{\ell} \quad , \tag{35}$$

$$\hat{T} = (\mathbf{BK})^T \left(\mathbf{C} + \alpha \mathbf{C}_{\mathbf{nn}}\right)^{-1} \left(\boldsymbol{\ell} - \mathbf{A}\hat{\mathbf{X}}\right) \quad , \tag{36}$$

and was obtained in (Moritz, 1980) as a solution of the variational problem

$$\mathbf{n}^T \mathbf{C}_{\mathbf{nn}}^{-1} \mathbf{n} + \alpha \|T\|^2 = \min \quad . \tag{37}$$

Here we introduce the following notations: α is the Tikhonov regularization parameter (Neyman, 1979; Moritz, 1980) or weight factor constraining the variability of the solution $\hat{T}$; $\|T\|$ is the norm of the potential T in a suitable Hilbert space with the kernel function $K(P, Q)$, which often allows the interpretation as a covariance function of the anomalous potential T; $\mathbf{B}$ is the linear operator from Eq. (29). The $(q \times q)$-matrix $\mathbf{C} = \mathbf{BKB}^T$ in Eq. (36) can be considered as the covariance matrix of $\mathbf{B}T$ in Eq. (28) and has the elements

$$C_{ij} = L_i^P L_j^Q K(P, Q) \quad , \tag{38}$$

where L_i^P and L_j^Q denote the linear operators L_i and L_j which are applied to the variable points P and Q, respectively. The $(q \times q)$-matrix $\mathbf{K}$ results from the kernel function $K(P, Q)$ or the basic covariance function of T, which agrees with our information about the Earth's gravity field in the studied area.

Thus we come to the solution (Eqs. 35 and 36) of Eq. (28) as a *solution* of the corresponding *variational problem* (Eq. 37) under the *least-squares principle*. The collocation method is defined here as a special version of Eq. (37), i.e. taking $\alpha = 1$ for the Tikhonov regularization factor. For the solution of Eq. (28) a priori information about the Earth's gravity field therefore has to be introduced, describing the behavior of the field which then is represented by the kernel function $K(P, Q)$.

For the practical application of Eqs. (35) and (36) the following problems have to be solved:

- The construction of an appropriate analytical kernel function $K(P, Q)$.
- The choice of a suitable parameter α, when applying the general case collocation with regularization.

In the next sections these problems are discussed with the further intention to construct a regional geoid in the Skagerrak area.

5 Reproducing kernels applied to collocation solutions

A classification of reproducing kernels $K(P,Q) = K^q(P,Q)$ according to their functional and physical significance was done by Marchenko and Lelgemann (1999) on the basis of the following general expression (Krarup, 1969):

$$K^q(P,Q) = \sum_{n=0}^{\infty} k_n^q \left(\frac{R_B^2}{r_P r_Q}\right)^{n+1} P_n(\cos\psi_{PQ}) = \sum_{n=0}^{\infty} k_n^q \left(\frac{r_{\tilde{Q}}}{r_P}\right)^{n+1} P_n(\cos\psi_{PQ}) \; . \qquad (39)$$

Here, $\tilde{Q}$ is a point obtained by the Kelvin transformation $r_{\tilde{Q}} = R_B^2/r_Q$ of the position Q of a measurement with respect to the Bjerhammar sphere with radius R_B (see also Hauck and Lelgemann, 1984); $P_n(\cdot)$ is the Legendre polynomial of degree n and ψ_{PQ} is the spherical distance between the radius-vectors r_P and r_Q. The coefficients k_n^q describe the asymptotic behavior of different kernels for $\sigma = R_B^2/r_P r_Q = r_{\tilde{Q}}/r_P$, that is (Neyman, 1979):

$$k_n^q = \frac{c}{n^{2(q-1)}} \sim \frac{1}{n^{2(q-1)}} \quad , \quad c = const, \qquad (40)$$

and q denotes the index of the corresponding Sobolev space H_2^q (do not confuse this index q with the number of observations in the last section). Sobolev spaces are complete subspaces of the general Hilbert space and therefore Hilbert spaces by themselves, namely Hilbert spaces with reproducing kernels $K^q(P,Q)$.

If the coefficients k_n^q are chosen properly, closed analytical expressions can be obtained for the kernel which is particularly suitable for practical applications. As shown in the Table 1, the reproducing kernels applied in physical geodesy can be described by singular harmonic functions. It is remarkable that they can be subdivided into two parts:

- if $(0 \le q \le 1)$ the reproducing kernels are described by singular point harmonic functions from zero up to second degree, representing a pole (point mass) a dipole and a quadrupole potential, respectively.
- if $(1.5 \le q \le 2.5)$ the kernel function can be interpreted by special combinations of line harmonic functions with different laws of line density distribution of the form $\nu = r^{A-1}$, forming two classes according whether $(A \le 0)$ or $(A > 0)$.

The asymptotic, which corresponds to the reproducing kernel $K^q(P,Q)$ with $q = 3/2$ (see Table 1), is in agreement with G. Darwin's (1884) law of density.

In further computations we will use reproducing kernels, which are described only by *singular point harmonic functions*. In this case, by the application of Kelvin transformation to the potential of multipoles (Marchenko, 1987) the expressions for the corresponding kernel functions can be obtained in the form

$$K_m(\sigma,\psi) = c \sum_{n=m}^{\infty} \binom{n}{m} \sigma^{n+1} P_n(\cos\psi_{PQ}) \quad , \qquad (41)$$

Class (Type of the singularity)	Author	$\tilde{k}_n^q = \frac{k_n^q}{c}$	Index q of the Hilbert space H_2^q
Radial Multipoles			
Radial quadrupole	Marchenko, 1987	$\tilde{k}_n^q = \binom{n}{2}$	$q = 0$
Radial dipole	Hauck and Lelgemann, 1984	$\tilde{k}_n^q = n$	$q = 0.5$
Pole (point mass)	Krarup, 1969	$\tilde{k}_n^q = 1$	$q = 1$
Finite radial straight lines with the density $\nu = r^{A-1}$			
$A = 0$	Moritz, 1980	$\tilde{k}_n^q = 1/n$	$q = 1.5$
$A = 1$	Hauck and Lelgemann, 1984	$\tilde{k}_n^q = 1/(n+1)$	$q = 1.5$
$A = 0$, $A = -1$	Tscherning, 1972	$\tilde{k}_n^q = 1/n(n-1)$	$q = 2$
A=-1, A=-2	Lauritzen, 1973	$\tilde{k}_n^q = 1/(n-1)(n-2)$	$q = 2$
A=-1, A=-2, A=+B	Tscherning and Rapp, 1974	$\tilde{k}_n^q = 1/(n-1)(n-2)(n+B)$	$q = 2.5$

Table 1: Various kernels used in geodetic applications (Marchenko and Lelgemann, 1999)

where the spectral coefficients are given by the binomial coefficients. For q one gets $q = 1 - m/2$. For $m = 0$ we get the set $k_n^q = 1$ (*Krarup's kernel*; potential of a simple pole or point mass, respectively):

$$K_0(\sigma, \psi) = c\,\sigma \sum_{n=0}^{\infty} \sigma^n P_n(\cos\psi_{PQ}) = \frac{\sigma}{L} \quad , \quad L = \sqrt{1 + \sigma^2 - 2\sigma\cos\psi_{PQ}} \quad , \qquad (42)$$

and for $m = 1$ the set $k_n^q = n \quad (n > 0)$ (*Poisson's kernel without term of the degree zero*; potential of a dipole):

$$K_1(\sigma, \psi) = c\,\sigma \sum_{n=1}^{\infty} n\,\sigma^n P_n(\cos\psi_{PQ}) = \frac{1}{2}\left[\frac{\sigma(1-\sigma^2)}{L^3} - \frac{\sigma}{L}\right] \quad . \qquad (43)$$

Closed expressions for all other point harmonic kernels K_m (kernels corresponding to radial multipoles) can be obtained recursively (Marchenko, 1998):

$$\begin{aligned} mK_m(\sigma,\psi) &= c\left[(2m-1)\ \frac{K_1(\sigma,\psi)}{K_0(\sigma,\psi)}\ K_{m-1}(\sigma,\psi)\right. \\ &\left. -\ (m-1)\ K_0(\sigma,\psi)\ K_0(\sigma,\psi)\ K_{m-2}(\sigma,\psi)\right] \quad . \end{aligned} \tag{44}$$

and can be computed by use of the initial values resulting from Eqs. (42) and (43). Thus, all functions $K_m(P,Q)$ are nothing else but certain combinations of the reproducing kernels $K_0(P,Q)$ and $K_1(P,Q)$, characterized by the property that the solid spherical harmonics from degree zero up to $(m-1)$ are not included.

Practical evaluations of the point reproducing kernels for basic and cross-covariance functions (in least squares-collocation) can be found in Marchenko, Abrikosov (1994) and Marchenko (1998, Section 15.2) in detail.

6 On the choice of a regularization parameter α

A solution (Eqs. 35, 36) of the variational problem (Eq. 37) requires a choice of the regularization parameter α. According to Moritz (1980) this choice corresponds to a different weighting between the square of the function norm $\|T\|^2$, and of the error norm $\mathbf{n}^{\mathrm{T}}\mathbf{C}_{nn}^{-1}\mathbf{n}$ and, by this, one selects the degree of smoothing of the potential field T. A larger factor α means a stronger smoothing of the solution and attributes more variation to the noise vector $\hat{\mathbf{n}}$.

The collocation requires the inversion of a matrix with a dimension equal to the number of observations, therefore any iterative process for an optimum determination of α leads to a time consuming procedure if the number of observations is large. For this reason we use in this study two values of α for comparison:

$$\alpha = 1 \quad , \tag{45}$$

and

$$\alpha = 1 + \sqrt{1 + \frac{Trace\,(\mathbf{C}\ \mathbf{C_{nn}})}{Trace\,(\mathbf{C_{nn}}\mathbf{C_{nn}})}} \quad , \tag{46}$$

obtained by Abrikosov (1999) as the two extreme values fulfilling the following minimization problem

$$\left\|\mathbf{C_{nn}} - \hat{\mathbf{C}}_{\mathbf{nn}}(\alpha)\right\| = \min \quad , \tag{47}$$

where $\mathbf{C_{nn}}$ is the a priori ("true") covariance matrix and $\hat{\mathbf{C}}_{\mathbf{nn}}$ is the a posteriori covariance matrix, which is derived by applying the covariance propagation rule to the estimation $\hat{\mathbf{n}}$ of the vector $\mathbf{n}$ of measurement noise. In comparison with other approaches (Tikhonov and Arsenin, 1986; Morozov, 1987; Neyman, 1979, Scales,

1985), Eq. (46) admits the estimation of α prior to matrix inversion in Eqs. (35), (36) presupposed that the kernel function $K(P,Q)$ was derived in good agreement with the initial information about the regional gravity field. Thus the relationships of Eqs. (42)−(44) and (46) allow a solution according to Eq. (35) of the variational problem (Eq. 37) under the additional condition of Eq. (47), which leads for $\alpha = 1$ to a standard collocation solution and in the case of Eq. (46) to a solution which is called here *"collocation with regularization"*.

7 Geodetic application of potentials of eccentric multipoles

7.1 General remarks

In addition to the determination of the anomalous potential by a set of kernel functions (covariance functions) in Eqs. (35) – (38), we introduce another set of non-orthogonal functions and investigate their practical application to the solution of the gravity field approximation problem.

First, instead of the principal fundamental solution of Laplace's equation ($1/r$, where r with respect to the origin), we consider the set $\{1/r_i\}$, where r_i are the distances from the current point P to some non-centric points. These reciprocal distances are called the *non-central* fundamental solutions of Laplace's equation. Now we shall apply Maxwell's differentiation (Hobson, 1931; Marchenko, 1998) to the potentials $\{1/r_i\}$, introducing the nabla operator

$$\nabla' = \vec{i}'\frac{\partial}{\partial x'} + \vec{j}'\frac{\partial}{\partial y'} + \vec{k}'\frac{\partial}{\partial z'} \quad , \tag{48}$$

and the operator of differentiation with respect to the fixed multipole axes $\vec{h}_j^{\,i}$, $(j = 1, 2, ...n)$:

$$\frac{\partial}{\partial \vec{h}_j^{\,i}} = u_j^i\frac{\partial}{\partial x'} + v_j^i\frac{\partial}{\partial y'} + w_j^i\frac{\partial}{\partial z'} = \left(\vec{h}_j^{\,i}\cdot\nabla'\right) \quad . \tag{49}$$

We use the following notations in Eqs. (48) and (49): $\left(\vec{i}', \vec{j}', \vec{k}'\right)$ are the orthonormal base vectors in the local coordinate system $P_i(x'y'z')$ with the origin located currently at every fixed point P_i (see Fig. 2) of the set $\{1/r_i\}$; $\left(u_j^i, v_j^i, w_j^i\right)$ are the components of the axes (unit vectors) $\vec{h}_j^{\,i}$, $(j = 1, 2, ...n)$ of a special non-central point object.

Now, we apply the differential operator (Eq. 49) to the set $\{1/r_i\}$ of the potentials of multipoles of degree zero, located at an all-dense denumerable set of the fixed points $\{P_i\}$ that belongs to an auxiliary surface σ_A (Aleksidze, 1978). By this first differentiation we find the potentials $\{V_1^i\}$ of eccentric dipoles, which are associated with the same points (Fig. 2):

$$V_1^i = -M_1^i\frac{\partial}{\partial \vec{h}_1^{\,i}}\left(\frac{1}{r_1}\right) = -M_1^i\left(\vec{h}_1^{\,i}\cdot\nabla'\right)\frac{1}{r_i} \quad . \tag{50}$$

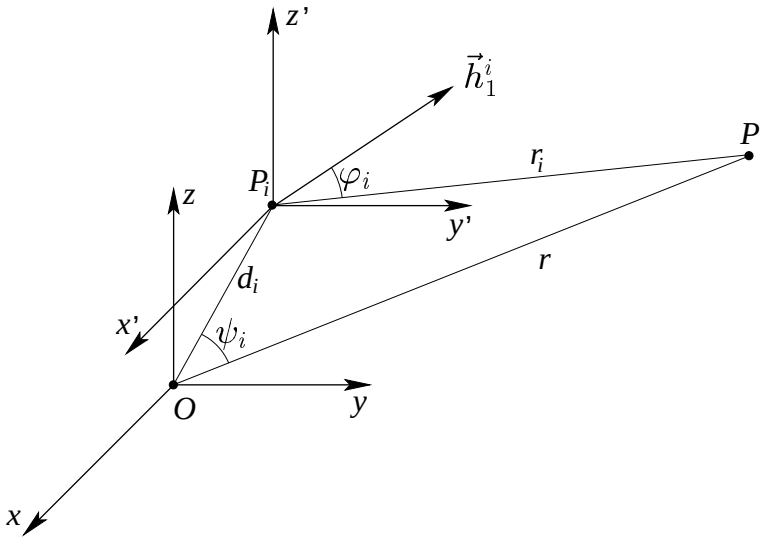

Figure 2: The local coordinate system $P_i(x'y'z')$ and non-central dipole with the axis $\vec{h}_1^i$

Secondly, by differentiating Eq. (50) we get the potentials $\{V_2^i\}$ of non-central quadrupoles, etc. Such a sequential differentiation according to Maxwell's method gives on the whole the generalization of Eq. (50). As a result, it is possible to associate these points $\{P_i\}$ with the potentials of non-central (eccentric) multipoles of the general kind of arbitrary degree n. There are different forms of their representation (Marchenko, 1987; Marchenko, 1998) which will not be discussed here.

Now the case $P_i(x'y'z') = O(xyz)$ is of special interest. Its application leads to a remarkable representation of standard solid spherical harmonics by a superposition of the two simplest potentials (Marchenko, 1998):

Any given solid spherical harmonic function V_n of degree n can be expressed by a certain combination of the fundamental solution of the Laplace equation (point mass potential) and the potentials of n central dipoles centered at the origin O of the coordinate system. The dipole axes coincide with the axes of the given solid spherical harmonic function V_n.

7.2 Potentials of radial multipoles and their essential parameters

As a matter of fact, the normalized potential $\tilde{v}_n^i = V_n^i/M_n^i$ of one non-central multipole of degree n has $2n$ linear-independent parameters, which characterize the directions of the n multipole axes $\left(\vec{h}_1^i, \vec{h}_2^i, ..., \vec{h}_n^i\right)$ (two parameters for one axis).

It would be very important for practical applications to find a simple analytical form for these base functions. For this purpose we consider the special case, when all n axes of each potential $\tilde{v}_n^i$ *have the same direction and coincide with the direction* $\overline{OP_i}$ (see Fig. 2). In this way, by Maxwell's differentiating in *radial* direction, we get the potential of the *radial* multipole

$$M_n^i \tilde{v}_n^i = (-1)^n \, \frac{M_n^i}{n!} \left(\vec{d}_i \cdot \nabla'\right)^n \left(\frac{1}{r_i}\right) = \frac{M_n^i}{n!} \, \frac{\partial^n}{\partial d_i^n} \left(\frac{1}{r_i}\right) \quad , \tag{51}$$

of degree n. In this case the direction of differentiation, the unit vector $\vec{d}_i/d_i$, coincides with the direction $\overline{OP_i}$ and has the following components

$$u_i = \frac{x_i}{d_i}, \; v_i = \frac{y_i}{d_i}, \; w_i = \frac{z_i}{d_i} \quad , \quad \left(u_i^2 + v_i^2 + w_i^2 = 1\right) \quad . \tag{52}$$

The parameter $d_i = \left|\vec{d}_i\right|$, the distance of the multipole from the origin, is contained in the basic expression for r_i (see Fig. 2):

$$r_i = \sqrt{r^2 + d_i^2 - 2rd_i \cos\psi_i} = \sqrt{(x - x_i)^2 + (y - y_i)^2 + (z - z_i)^2} \quad . \tag{53}$$

Now, a first differentiation leads to the potentials $\{\tilde{v}_1^i\}$ of radial dipoles ($n = 1$), located at the points $\{P_i\}$:

$$\tilde{v}_1^i = -\left(\vec{d}_i \cdot \nabla'\right) \frac{1}{r_i} = \frac{\partial}{\partial d_i} \left(\frac{1}{r_i}\right) = \frac{r\cos\psi_i - d_i}{r_i^3} = \frac{\cos\varphi_i}{r_i^2} \quad . \tag{54}$$

The expression (54) is given for the coordinate systems $O(xyz)$ and $P_i(x'y'z')$, respectively. On the other hand, taking into consideration Maxwell's rule of differentiation, we finally get

$$-\left(\vec{d}_i \cdot \nabla'\right) \tilde{v}_n^i = \tilde{v}_{n+1}^i \quad . \tag{55}$$

Eq. (55) describes the main property of the potential of a non-central radial multipole of degree n: every potential $\tilde{v}_n^i$ decreases proportionally to $r_i^{-(n+1)}$. Such a potential (without normalization) has only four parameters for each point P_i: the moment M_n^i and the three components (x_i, y_i, z_i) of this point. So, in case of radial multipoles we have only 2 axis-parameters (Eq. 52) instead of $2n$ for general multipoles without loss of the qualitative property of the potentials of multipoles (see Fig. 3). As a result, by sequential differentiating in accordance with Eq. (55) the following expression for normalized potentials of radial multipoles of an arbitrary n can be found:

$$\tilde{v}_n^i = \frac{P_n\left(\cos\varphi_i\right)}{r_i^{n+1}} \quad , \tag{56}$$

where $P_n\left(\cos\varphi_i\right)$ are the Legendre polynomials. The angle φ_i is connected with the local coordinate system $P_i\left(x'y'z'\right)$, (see Fig. 3). It can be proved that the basic recurrence formula for Legendre polynomials (Heiskanen and Moritz, 1967) can be used here for a straightforward computation of $\tilde{v}_n^i$ as well. As a result, we derive the recurrence formula

$$n\tilde{v}_n^i = (2n-1)\, r_i \tilde{v}_1^i \tilde{v}_{n-1}^i - (n-1)\, \tilde{v}_{n-2}^i \left(\frac{1}{r_i}\right)^2 \quad . \tag{57}$$

for the potentials $\tilde{v}_n^i$. Now starting from the potentials $\tilde{v}_0^i$ and $\tilde{v}_1^i$, the whole set of the potentials of radial multipoles from zero up to n degree can be calculated by Eq. (57).

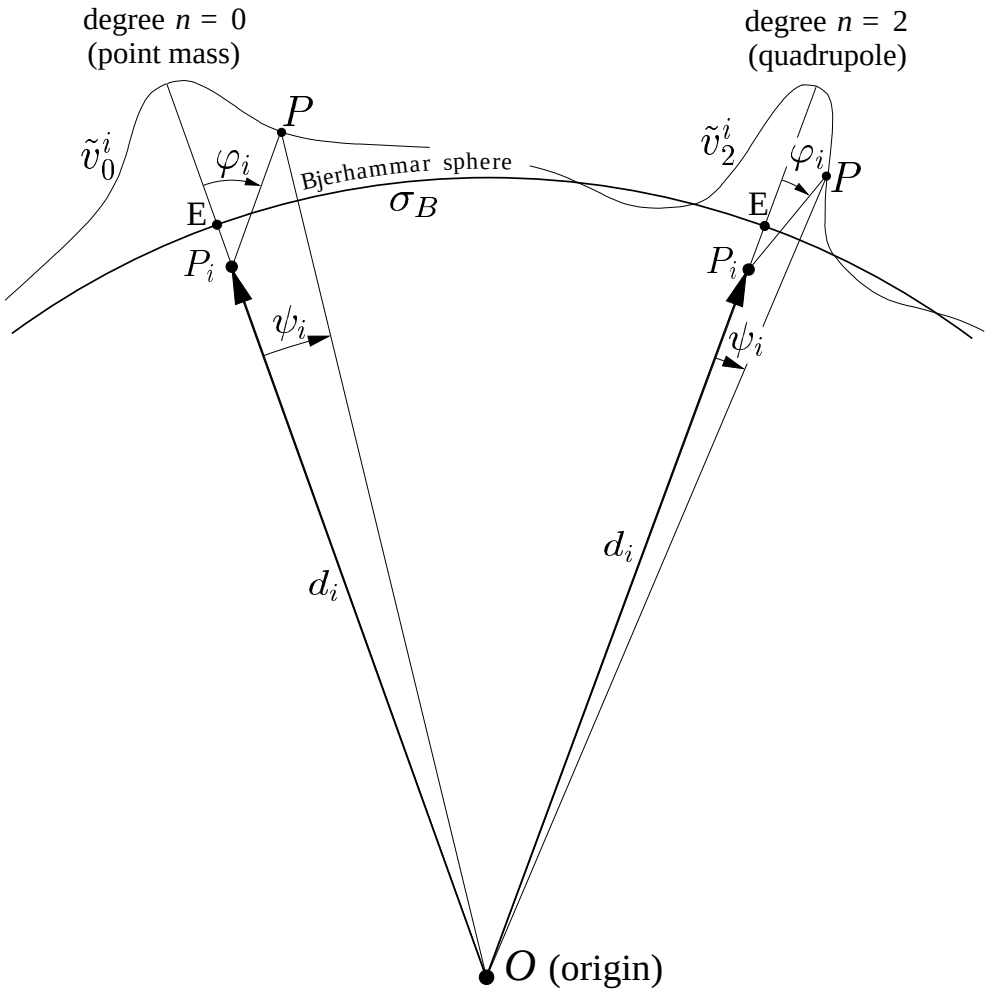

Figure 3: Sketch of the geometry for the potentials of two radial multipoles of different degrees ($n = 0$ and $n = 2$)

Obviously, the expansion of $\tilde{v}_n^i$ into a series of solid spherical functions can be written as

$$\tilde{v}_n^i = \sum_{k=n}^{\infty} \binom{k}{n} \frac{d_i^{k-n}}{r^{k+1}} P_k(\cos\psi_i) \quad . \tag{58}$$

where the standard formula for the binomial coefficients

$$\binom{k}{n} = \frac{k!}{n!\,(k-n)!} \quad , \tag{59}$$

is used.

A special study of the properties and the parameters of the potential $\tilde{v}_n^i$ of an arbitrary radial multipole was done especially regarding the Bjerhammar sphere σ_B in (Marchenko, 1987, 1998). The *first essential parameter* or the *magnitude* of $\tilde{v}_n^i$ at the epicenter E (see Fig. 3) follows from the value of $\tilde{v}_n^i$ at the point E:

$$\tilde{v}_n^i(\psi_i = 0) \;=\; \tilde{v}_n^i(\varphi_i = 0) \;=\; \tilde{v}_n^i(E) \;=\; \frac{1}{R_B^{n+1}(1-h_i)^{n+1}} \quad , \quad h_i = \frac{d_i}{R_B} \quad , \qquad (60)$$

because the potential of a radial multipole of degree n has its global maximum at E, since everywhere on σ_B the following inequality is valid $\tilde{v}_n^i(\cos\varphi_i = 1) > \tilde{v}_n^i(\cos\varphi_i \neq 1)$, and its global minimum at the antipodal point E'. It is evident that the local behavior of $\tilde{v}_n^i$ can be described additionally by the *second essential parameter* ξ_n (called here: "*decreasing length*") of the potential of the radial multipole

$$\tilde{v}_n^i(\psi_n = \xi_i) \;=\; \frac{1}{2}\,\tilde{v}_n^i(\psi_i = 0) \;=\; \frac{1}{2\,R_B^{n+1}(1-h_i)^{n+1}} \quad , \qquad (61)$$

because any function $\tilde{v}_n^i(0)$ has a maximum at the point $E(\psi_i = 0)$. The curvature $k_n(\varphi_i = 0)$ of the curve $\tilde{v}_n^i = \tilde{v}_n^i(\psi_i)$ at the epicenter E may be adopted as a *third essential parameter* of $\tilde{v}_n^i$ for $(\psi_i = 0)$. The corresponding expression in the closed form depends essentially not only on h_i, but on the degree n as well

$$k_n(E) \;=\; k_n(\varphi_i = 0) \;=\; -\left.\frac{d^2\tilde{v}_n^i}{d\psi_i^2}\right|_{\psi_i=0} \;= \frac{(n+1)(n+2h_i)}{R_B^{n+1}\,2(1-h_i)^{n+3}} \quad . \qquad (62)$$

These parameters $\tilde{v}_n^i(\psi_i = 0)$, ξ_n, $k_n(E)$ represent three excellent characteristics of the local structure of $\tilde{v}_n^i$. Note finally that their definition is identical to H. Moritz (1980) definition of the *essential parameters of covariance functions*: the variance, the correlation length, and the curvature parameter. This is no surprise because the local properties of the functions $\tilde{v}_n^i$ are similar to the local properties of covariance functions of the anomalous potential T. Moreover, these functions were used successfully in Section 4 for the creation (by means of Kelvin transformation) of the corresponding reproducing kernels.

Next, we need to use the following assertion (Marchenko, 1998), which has a direct connection to the Runge-Krarup theorem (Krarup, 1969):

The set $\{\tilde{v}_0^i\}$ *of the potentials of eccentric radial multipoles of degree zero (i.e. potentials of point masses with sum of all masses being equal to zero, i.e. no degree zero solid spherical harmonic) and the set* $\{\tilde{v}_1^i\}$ *of the potentials of eccentric dipoles are non-orthogonal base systems in the Hilbert space* $H_2^q(\Sigma)$. *On the whole, every set of the potentials* $\{\tilde{v}_n^i\}$, *if* $n > 1$, *is a linear independent and complete base system on any subset of* $H_2^q(\Sigma)$ *not including all linear combinations of solid spherical harmonics from zero up to degree* $n-1$.

Thus, there is a possibility of the approximation of the anomalous potential T by these (suitable) non-orthogonal *potential functions* in the domain Σ outside the Bjerhammar sphere σ_B.

$$T(P) = \sum_{i=1}^{\infty} M_n^i \tilde{v}_n^i(P) \quad . \qquad (63)$$

7.3 Approximation of geodetic functionals

Now, for practical applications we introduce according to (Marchenko and Abrikosov, 1994) a dimensionless potential $\hat{v}_n^i$ of radial multipole of n-degree as

$$\hat{v}_n^i = \tilde{v}_n^i \, r^{n+1} \quad , \tag{64}$$

which is located at the same point P_i. Substituting Eq. (64) into Eq. (56) we get

$$\hat{v}_n^i = \left(\frac{r}{r_i}\right)^{n+1} P_n\left(\cos\varphi_i\right) \quad . \tag{65}$$

Then, the expansion in Eq. (63) in view of Eq. (64) can be rewritten as

$$T(P) = \sum_{i=1}^{\infty} \frac{m_i^{(n)}}{r^{n+1}} \, \hat{v}_n^i(P) \quad , \tag{66}$$

where $m_i^{(n)}$ are some coefficients or the multipole moments; r is the *geocentric* distance of an external point P. On the whole, we assume also that for each potential $\hat{v}_n^i$ an appropriate degree $n = n_i$ associated with the point P_i can be chosen.

Next, we shall derive several expressions for some geodetic functionals. First we represent the geoid undulations as

$$N(P) = \frac{1}{\gamma_P} \sum_{i=1}^{K} \frac{m_i^{(n)}}{r^{n+1}} \, \hat{v}_n^i(P) \quad , \tag{67}$$

and the gravity anomalies as

$$\Delta g(P) = \sum_{i=1}^{K} \frac{m_i^{(n)}}{r^{n+2}} \, g_n^i(P) \quad , \tag{68}$$

as well as any other linear geodetic functionals. The functions $g_n^i = g_n^i\,(P)$ can be obtained from the fundamental equation of physical geodesy (Eq. 6, here in spherical approximation) as

$$g_n^i(P) = s_i \, \frac{\partial v_n^i(P)}{\partial s_i} + (n-1)\, v_n^i(P) \quad , \tag{69}$$

where s_i is the relative geocentric distance of a multipole at the point P_i:

$$s_i = \frac{d_i}{r} \quad . \tag{70}$$

Then inserting Eqs. (64) and (70) into the recurrence formula (Eq. 57), after suitable manipulations we get the recurrence formulae especially for Eqs. (66), (67), and (68) separately

$$\begin{aligned} n\, q_i^2 \, \hat{v}_n^i &= (2n-1)\left(\cos\psi_i - s_i\right) \hat{v}_{n-1}^i - (n-1)\, \hat{v}_{n-2}^i, \\ \hat{v}_0^i &= \frac{1}{q_i}, \end{aligned} \tag{71}$$

$$
\begin{aligned}
n\, q_i^2 \frac{\partial \hat{v}_n^i}{\partial s_i} &= (2n-1)\,(\cos\psi_i - s_i)\,\frac{\partial \hat{v}_{n-1}^i}{\partial s_i} - (n-1)\,\frac{\partial \hat{v}_{n-2}^i}{\partial s_i} + \\
&\quad +2n\,(\cos\psi_i - s_i)\,\hat{v}_n^i - (2n-1)\,\hat{v}_{n-1}^i, \qquad (72) \\
\frac{\partial \hat{v}_0^i}{\partial s_i} &= \frac{\cos\psi_i - s_i}{q_i^3}, \\
q_i &= \sqrt{1 + s_i^2 - 2 s_i\,\cos\psi_i} \quad . \qquad (73)
\end{aligned}
$$

It is evident that a practical application of these last expressions requires a solution of the special inverse problem (Marchenko, 1998): "For a given set of geodetic measurements (treated before as linear functionals of the anomalous potential T) we want to find some appropriate (and approximating) finite set of radial multipoles i.e. the values of moments, locations, and degrees for the further approximation of T in the frame of a *linear problem only.*"

For the choice of coordinates of the potentials $(\tilde{v}_0^i)$ of point masses various approaches exist (see, for instance, Barthelmes, 1980, 1982, 1986, 1988; Meshcheryakov and Marchenko, 1980; etc.).

Note now, that the considered essential parameters lead to the additional possibility to compute the geocentric distances d_i of $(\tilde{v}_n^i)$. Actually, by estimating the empirical value ξ^{emp} of the decreasing length from a preliminary analysis of the initial data we can solve this problem on the basis of the 2nd essential parameter ξ_n analytically for $n = 0$, $v_0^i = 1/r_i$. Thus, substituting ξ^{emp} into Eq. (61) instead of ξ_0 we come to the relationship $(n = 0)$:

$$
h_i = \frac{4}{3} - \frac{1}{3}\left(\cos\xi^{emp} + \sqrt{\cos^2\xi^{emp} - 8\cos\xi^{emp} + 7}\right) \quad , \quad (n=0) \quad , \qquad (74)
$$

for the relative geocentric distance h_i of a separate point mass.

In addition to this example, we may try further to determine an optimal degree n of the potentials $\hat{v}_n^i$. This problem can be solved also by means of the essential parameters of $\hat{v}_n^i$. Some approaches were realized before as the so-called preliminary multipole analysis (PMA), (Marchenko, 1987) and the sequential multipole analysis (SMA), (Marchenko, Abrikosov, 1994). Both the PMA and SMA techniques use initial data of the same type only. The idea of the SMA to find the horizontal positions (long. and lat.) of the multipoles is the same as used for point masses in (Barthelmes, 1980, 1982, 1983, 1986, 1988). As an example we describe one step of the SMA algorithm, which contains the following sub-steps.

1. Input of the the initial set of the gravity data; $i = 1$.
2. Find the largest absolute value (maximum or minimum) of the gravity data (step i); postulate this extremum as the epicenter E of the i-th radial multipole with the polar coordinates (ϑ_i, λ_i); estimate the *empirical values* of essential parameters.
3. Determine the multipole parameters s_i, n and $m_i^{(n)}$ by means of these coordinates (ϑ_i, λ_i) and Eqs. (60) – (62) or Eqs. (75) – (78).

4. Compute the transformed data by removing the contribution of the potential of the i-th multipole from the initial data.
5. Put $i = i + 1$ and return to step 2 if the desired accuracy is not achieved.

The relative distance s_i, the degree n and the moment $m_i^{(n)}$ of one multipole (located at the point P_i) may be determined on the basis of the *empirical "isotropic" (i.e. independent of the azimuth) function* (EIF), (Marchenko, 1987). We introduce the EIF as any discrete function of the spherical distance ψ_i, which is computed by means of an *averaging of the initial data over the azimuth.* The EIF can be computed locally inside a suitable spherical zone around the chosen epicenter (E). The empirical local parameters of the EIF (by analogy to the parameters $\tilde{v}_n^i\,(\psi_i = 0)$, ξ_n, $k_n(E)$) can be determined numerically from the closest approximation of the EIF by one of the analytical expressions for $\hat{v}_n^i$ with a certain optimal degree. As a result, the approximation of the gravity field around a selected local extremum is provided by the analytical "isotropic" function (AIF), AIF=$\hat{v}_n^i$ for every step.

Thus, the base functions $\hat{v}_n^i$ and g_n^i lead to the following analytical expressions of these essential parameters. *The magnitudes at the epicenter are*:

$$v_n^i(\psi_i = 0) = \left(\frac{1}{1 - s_i}\right)^{n+1}, \quad g_n^i(\psi_i = 0) = \frac{n + 2s_i - 1}{(1 - s_i)^{n+2}} \quad . \tag{75}$$

The decreasing length is:

$$f_n^i(\psi_i = \xi) = \frac{1}{2}\, f_n^i(\psi_i = 0) \quad , \tag{76}$$

where f_n^i corresponds to one of the geodetic functionals represented here in the form of Eq. (66) or Eq. (67) or Eq. (68), etc. Eq. (76) is non-linear with respect to s_i. It is obvious from Eqs. (75) and (76) that the multipole moment $m_i^{(n)}$ does not appear in these equations which leads to the determination of s_i *independently* from $m_i^{(n)}$.

The curvatures $k_n(E)$ *for* $(\psi_i = 0)$ *are*:

$$\left.\frac{\partial^2 v_n^i}{\partial \psi_{iP}^2}\right|_{\psi_i = 0} = -\frac{(n+1)(n+2s_i)}{2(1 - s_i)^{n+3}} \quad , \tag{77}$$

$$\left.\frac{\partial^2 g_n^i}{\partial \psi_{iP}^2}\right|_{\psi_i = 0} = -\frac{n+1}{2(1 - s_i)^{n+3}}\left[2s_i + (n + 2s_i)\left(n - 1 + \frac{n+3}{1 - s_i}\right)\right] \quad . \tag{78}$$

Thus, the determination of the multipole parameters can be realized (sub-step 3 mentioned before) in the following way:

- $n = 0$; Input of the empirical essential parameters of the EIF (magnitude, decreasing length, curvature and coordinates (ϑ_i, λ_i) as well).
- Determine s_i by means of the empirical decreasing length ξ^{emp} (with the fixed degree n).

- Determine the multipole moment $m_i^{(n)}$ for fixed s_i and n; computations may be based either on the magnitude of the EIF at the epicenter (and the curvature) or on the local least-squares approximation of the gravity field by one potential $\hat{v}_n^i$.
- Put $n = n + 1$ and return to point 2, if the optimal degree n is not achieved.

So, this procedure is an appropriate realization of the point 3 of the SMA algorithm, which is based on the local properties of $\hat{v}_n^i$ only. As a result, we can establish an optimal degree n and $(d_i, \vartheta_i, \lambda_i, m_i^{(n)})$ of the radial multipole: either from the iterative non-linear fitting of the EIF by the AIF or from the closest approximation of the gravity data locally (around the epicenter). Again the next step of such an optimization is the final total least-squares re-adjustment of the whole set $\{m_i^{(n)}\}$ in the frame of a *linear problem.* Another version is the re-adjustment of certain subsets of $\{m_i^{(n)}\}$ during the SMA process.

As a result, the application of radial multipoles for the approximation of the Earth's gravity field in some area (local, regional or global) may include the following steps.

1. Preparation of heterogeneous initial data sets for creation of a homogeneous gravity data set (e.g. by inversion of the altimeter data to gravity anomalies, etc.).
2. Preliminary construction of the gravity model (Eq. 66) by applying the SMA technique.
3. Final total re-adjustment of the multipole moments $\{m_i^{(n)}\}$ for all sets of heterogeneous data.

Thus, a solution of the mentioned special inverse problem leads to an approximation of the Earth's regional gravity field by non-orthogonal harmonic functions and is based here on their analytical representation by a set of potentials of eccentric radial multipoles.

8 Airborne-only and airborne/UEGN94 combined geoid solutions

To illustrate geoid computations on the basis of airborne point gravity anomalies in the Skagerrak area at a $(3' \times 3')$ grid, let us consider solutions of this problem in the frame of the approaches described above. First, we start from the operational approach where the following basic methods were applied:

- Collocation method (Eqs. 35, 36 with $\alpha = 1$)
- Collocation with regularization (Eqs. 35, 36 and 46)

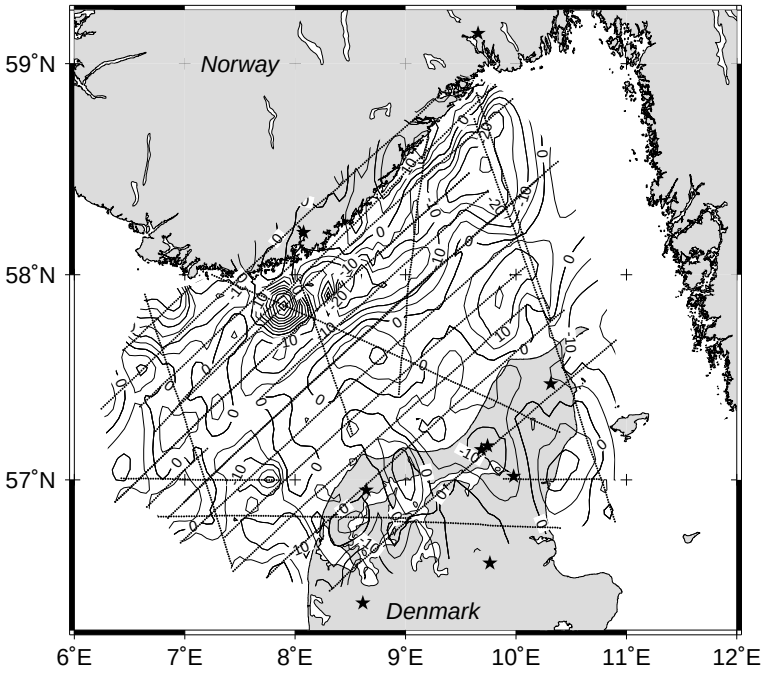

Figure 4: Differences $\delta\Delta g$ between the initial airborne and EGM96 (360,360) gravity anomalies Δg (3370 point values) in the Skagerrak area; contour interval: 5 mGal; 9 points of UEGN94 gravimetric network are shown by asterisks

Statistics (3370 points)	Minimum	Maximum	Mean	rms	Standard deviation
Initial airborne Δg Set 1 of 3370 points	-48.6	48.9	-3.2	13.9	13.5
$\delta\Delta g = (\Delta g - \Delta g_{\mathrm{EGM96}})$	-36.8	46.0	-2.5	9.7	9.4

Table 2: Statistics of the point Δg and residual $\delta\Delta g$ airborne gravity anomalies [mGal]

The following initial data sets in the Skagerrak area were used for further data processing:

- Set 1: 3370 airborne gravity anomalies (mean accuracy $\approx$ 2.4 mGal), which cover a part of the Skagerrak region;
- Set 2: 3379 gravity anomalies consisting of Set 1, supplemented by 9 points of UEGN94 absolute gravimetric network (mean accuracy $\approx$ 0.014 mGal), which are surrounding the Skagerrak area.

The "remove-restore" procedure was applied to remove the contribution of the long wavelength part of the Earth's global gravity field from every data set using the model EGM96 (360,360): $\delta\Delta g = \Delta g - \Delta g_{\mathrm{EGM96}}$ (Table 2). In order to avoid extrapolation, grid values were predicted only for the area covered by observations (Fig. 4).

As a result, the prediction of geoid heights δN were made for each set separately. After solving this basic problem, the predicted geoid undulations were restored by means of the EGM96 model: $N = \delta N + N_{\mathrm{EGM96}}$. Because the mean height of the predicted points is smaller than 10 m and the main part of the initial values of Δg represents only airborne gravity anomalies, an application of terrain corrections was omitted.

The *empirical covariance function* (ECF) was constructed (Table 3) on the basis of the residual gravity anomalies $\delta\Delta g$ (Fig. 4) for the mean surface of their location. Then, this ECF was approximated by some reproducing kernels or *analytical covariance functions* ACF, derived in Section 5 from radial multipole potentials by the Kelvin transformation, that provides the covariance propagation in $\mathbf{R}^3$ to geoid heights and other functionals of the anomalous potential.

The following ACF's were sufficient for an application in the Skagerrak area:

1. ***Poisson*** kernel without harmonic of zero degree, which corresponds to radial ***dipole kernel*** (Table 4, Fig. 5).
2. Special combination of ***Krarup/Poisson*** kernels without harmonic of zero and first degrees, which corresponds to radial ***quadrupole kernel*** (Table 4).

Because of the slightly better fit of the dipole kernel, this one was selected for the following solutions.

Region	Variance [mGal^2]	Correlation length [degree]	Parameter of Curvature
Skagerrak	88.5421	0.122416	2.2618

Table 3: Essential parameters of empirical covariance function, constructed for the mean surface of airborne gravity anomalies (altitude $\approx$ 400m)

ACF	Degree m	Scale-factor c in Eq. (44) $[m^2/s^2]$	Bjerhammar sphere radius [meters]	Relative accuracy of ECF-fit [%]	Correlation length [degree]	Parameter of Curvature
Dipole kernel	1	$1.8257 \cdot 10^{-20}$	6344724.87	9.9	0.125221	3.2680
Quadrupole kernel	2	$1.9218 \cdot 10^{-22}$	6339266.01	10.0	0.129568	3.1339

Table 4: Parameters of the analytical covariance functions, constructed for the mean surface of airborne gravity anomalies (altitude $\approx$ 400m)

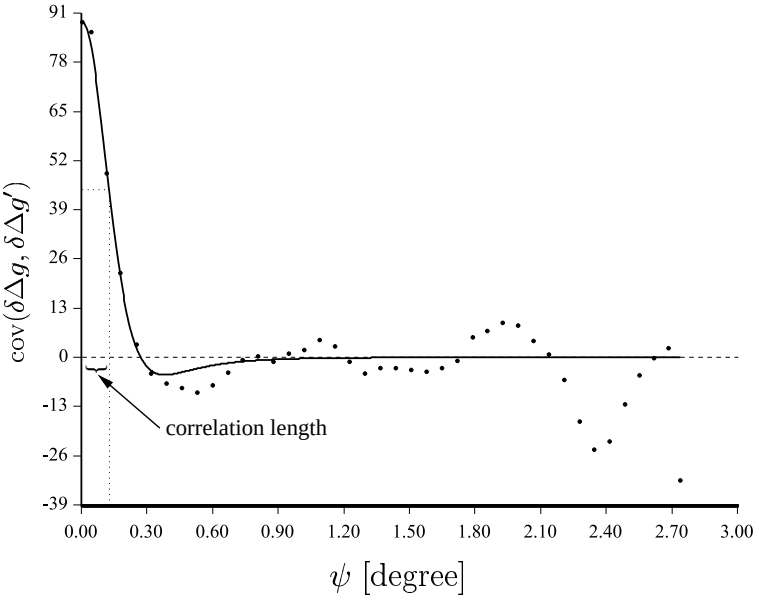

Figure 5: Empirical (ECF) (dotted) and analytical (ACF) (solid) covariance functions [mGal^2], based on 3370 airborne $\delta\Delta g = (\Delta g - \Delta g_{\mathrm{EGM96}})$; analytical function represented by ***dipole*** kernel.

To illustrate the results of geoid prediction by collocation and regularization techniques we introduce the following abbreviations:

- AC1: Collocation solution for airborne geoid, based on Set1;
- AC2: Collocation solution for airborne/UEGN94 geoid, based on Set2 (Fig 6);
- AR1: Regularization solution for airborne geoid, based on Set1;
- AR2: Regularization solution for airborne/UEGN94 geoid, based on Set2 (Fig 7).

The resulting geoids AC2 and AR2 shown in Figs. (6) and (7) were compared with the solution of Forsberg (2000), computed for the Nordic countries, which is an improved version of the geoid of Forsberg et al. (1997), now including the aerogravimetry data also used in this study. As a result, Tables (6, 7) and Figs. (8, 9) reflect this independent comparison and we come to the conclusions:

1. Including only 9 points of the UEGN94 absolute gravimetric network leads to a better agreement in terms of the mean difference of the solutions AC2 and AR2 with Forsberg's geoid,
2. Application of the regularization method based on Eq. (35), and Eq. (36) with a relatively large value of $\alpha \approx 5$ for the regularization parameter deduced according to Eq. (46) provides smaller rms differences between the predicted geoid heights rather than standard collocation ($\alpha = 1$) with the same reproducing kernel (Tables 6, 7).
3. In view of the rms values, this conclusion holds for both the solutions including and excluding the additional information from the UEGN94 gravimetric network.

Statistics	Minimum	Maximum	Mean	rms	Standard deviation
Collocation method: Solution AC2					
Predicted geoid undulations N	36.6809	41.6638	39.3877	39.4048	1.1605
Regularization method: Solution AR2					
Predicted geoid undulations N	36.7470	41.6417	39.3867	39.4035	1.1509
Differences between two solutions					
AR1 - AC1	-0.1006	0.0932	-0.0004	0.0189	0.0189
AR2 – AC2	-0.1007	0.0925	-0.0010	0.0189	0.0189

Table 5: Statistics for final versions of airborne/UEGN94 geoids [m], computed at 3271 grid points ($3' \times 3'$)

Statistics of differences dN (3271 points)	Minimum	Maximum	Mean	rms	Standard deviation
Collocation method: Solution AC1 ($\alpha = 1$)					
dN = Forsberg's grid values $N-$ predicted N	-0.1914	0.1876	0.0123	0.0534	0.0520
Regularization method: Solution AR1 ($\alpha = 5.0724$)					
dN = Forsberg's grid values $N-$ predicted N	-0.1914	0.1772	0.0127	0.0467	0.0449

Table 6: Differences dN between Forsberg's geoid grid ($3' \times 3'$) and the predicted values [m] based only on 3370 airborne gravity anomalies

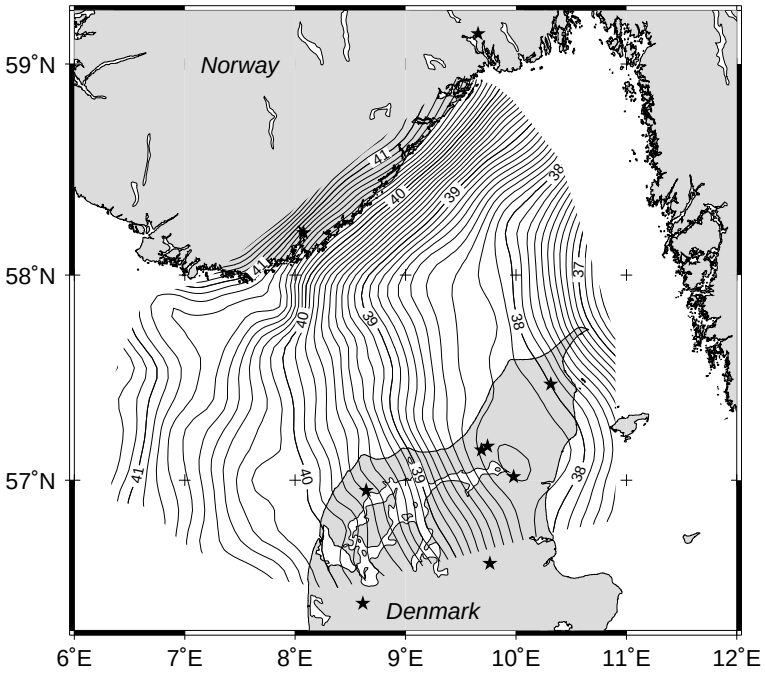

Figure 6: Airborne/ UEGN94 geoid solution AC2, based on the collocation method with dipole kernel; contour interval: 0.1 m; 9 points of UEGN94 network are shown by asterisks

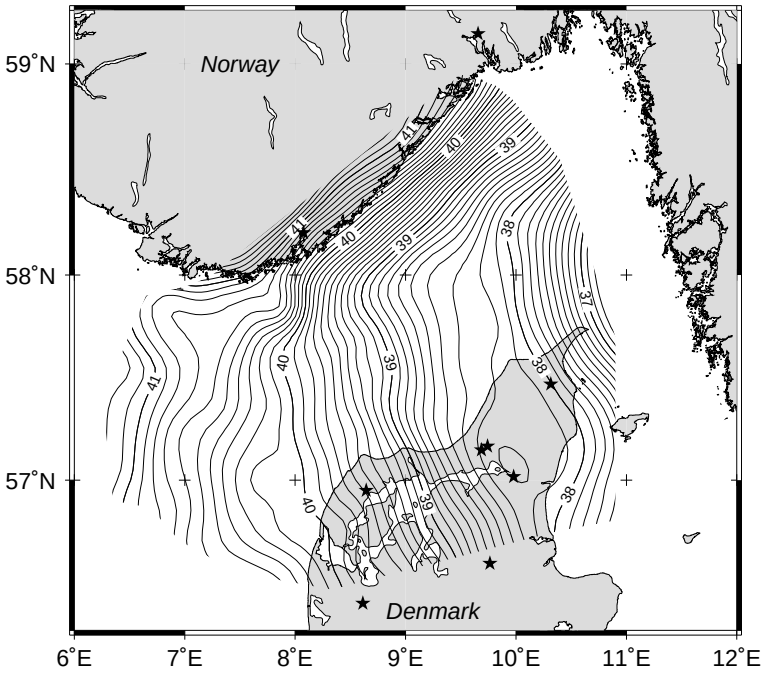

Figure 7: Airborne/ UEGN94 geoid solution AR2, based on the regularization method with dipole kernel; contour interval: 0.1 m; 9 points of UEGN94 network are shown by asterisks

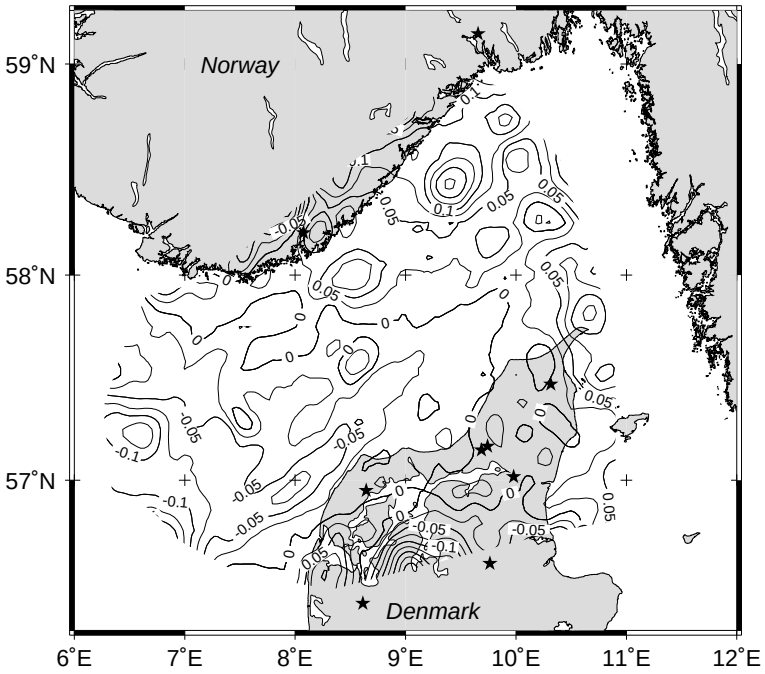

Figure 8: Differences between AC2 geoid, based on the collocation method with dipole kernel and Forsberg's geoid grid ($3' \times 3'$); contour interval: 0.025 m; 9 points of UEGN94 network are shown by asterisks

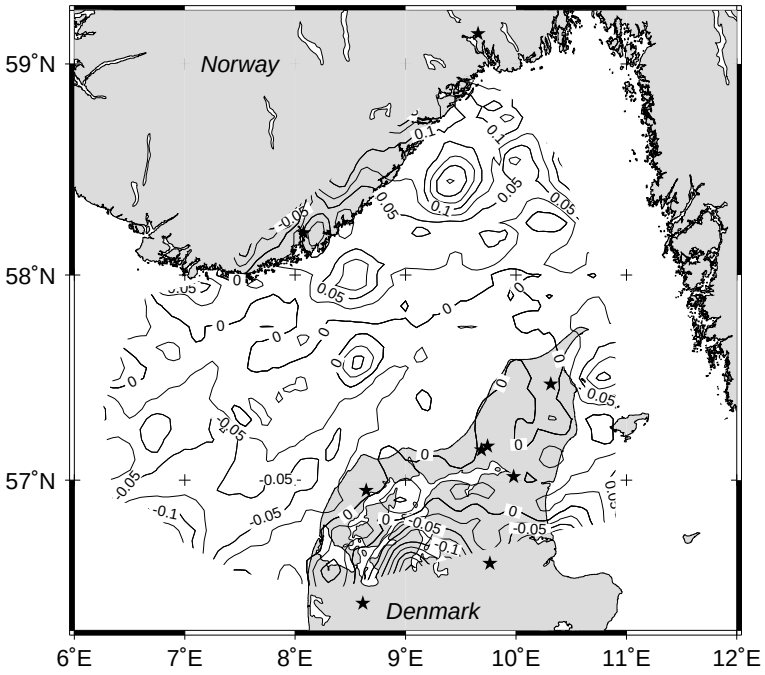

Figure 9: Differences between AR2 geoid, based on the regularization method with dipole kernel and Forsberg's geoid grid ($3' \times 3'$); contour interval: 0.025 m; 9 points of UEGN94 network are shown by asterisks

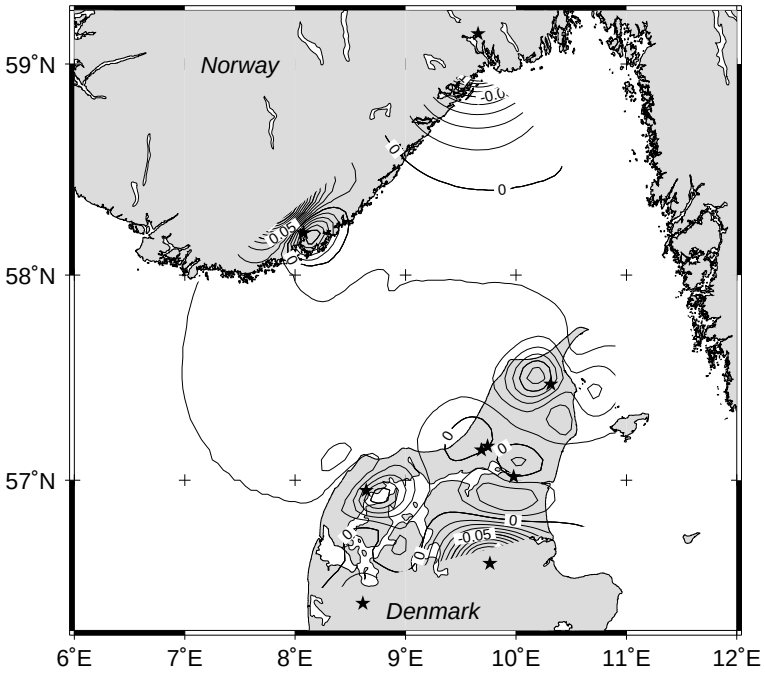

Figure 10: Contribution of 9 points of UEGN94 network (asterisks) to geoid AC1: differences of solutions AC2 minus AC1; contour interval: 0.01 m

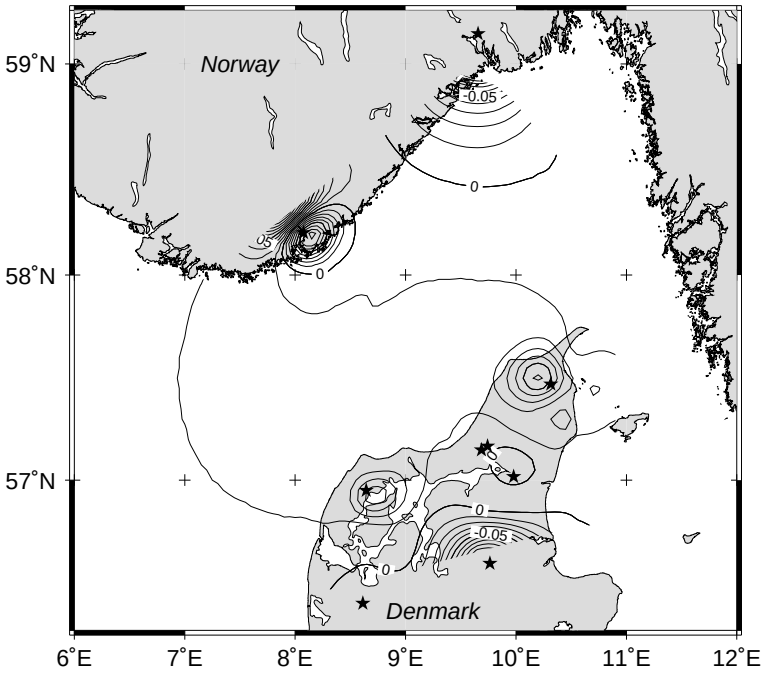

Figure 11: Contribution of 9 points of UEGN94 network (asterisks) to geoid AR1: differences of solutions AR2 minus AR1; contour interval: 0.01 m

Statistics of differences dN (3271 points)	Minimum	Maximum	Mean	rms	Standard deviation
Collocation method: Solution AC2 ($\alpha = 1$)					
dN = Forsberg's grid values $N-$ predicted N	-0.1957	0.1938	0.0049	0.0543	0.0540
Regularization method: Solution AR2 ($\alpha = 5.0724$)					
dN = Forsberg's grid values $N-$ predicted N	-0.1914	0.1774	0.0059	0.0480	0.0476

Table 7: Differences dN between Forsberg's geoid grid ($3' \times 3'$) and the predicted values [m] based on 3379 gravity anomalies, including 9 points of the UEGN94 gravimetric network

Statistics	Minimum	Maximum	rms
Collocation method: Solution AC1	0.051	0.147	0.066
Regularization method: Solution AR1	0.052	0.148	0.069
Collocation method: Solution AC2	0.050	0.147	0.065
Regularization method: Solution AR2	0.052	0.148	0.068

Table 8: Accuracy estimation of the predicted geoid heights [m]

Statistics of differences dN (3271 points)	Minimum	Maximum	Mean	rms	Standard deviation
Collocation method					
Differences: sol. AC2−sol. AC1	-0.1129	0.1280	0.0074	0.0170	0.0153
Regularization method					
Differences: sol. AR2−sol. AR1	-0.1136	0.1163	0.0068	0.0167	0.0152

Table 9: Contribution [m] of 9 points of the UEGN94 network to geoid solutions AC2 and AR2

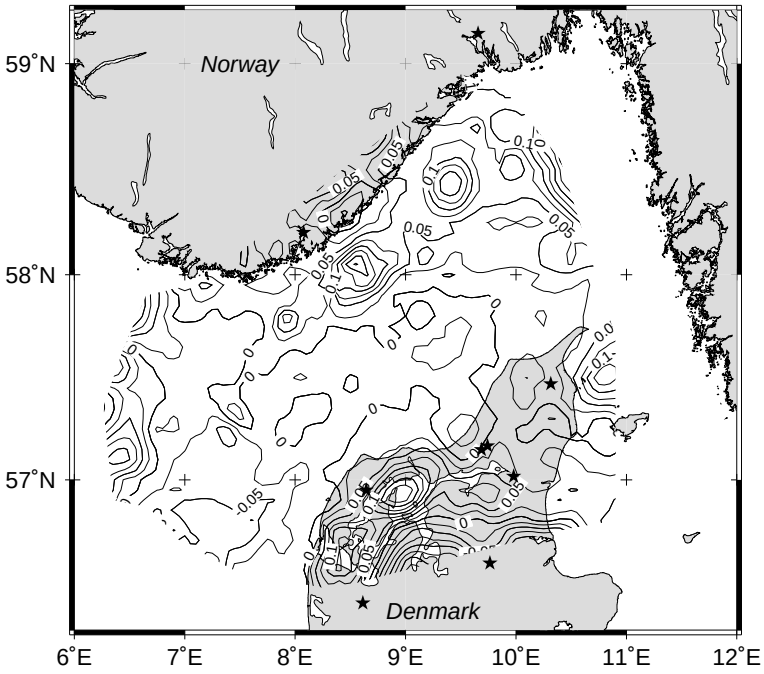

Figure 12: Differences between geoid SMA2, based on the approximation by radial multipole potentials, and Forsberg's geoid grid ($3' \times 3'$); contour interval: 0.025 m

Statistics of differences dN (3271 points)	Minimum	Maximum	Mean	rms	Standard deviation
Solution SMA1	-0.1850	0.2082	0.0221	0.0539	0.0491
Solution SMA2	-0.1653	0.2040	0.0196	0.0515	0.0476

Table 10: Differences dN between Forsberg's geoid grid ($3' \times 3'$) and the predicted values [m], based on the SMA1 and SMA2 regional models

---

The second part of airborne/UEGN94 geoid construction is based on the model approach where the parameterization (Eq. 66) of the anomalous potential T was fulfilled by means of:

- the radial multipole potentials of one chosen degree;
- a combination of radial multipole potentials of different degrees.

To illustrate the results of geoid prediction by means of Sequential Multipole Analysis (SMA) techniques we introduce new abbreviations:

- SMA1: SMA solution for airborne geoid (with application of multipoles from 1 up to 8 degrees), based on Set1;
- SMA2: SMA solution for airborne geoid (with application of multipoles from 1 up to 8 degrees), based on Set2.

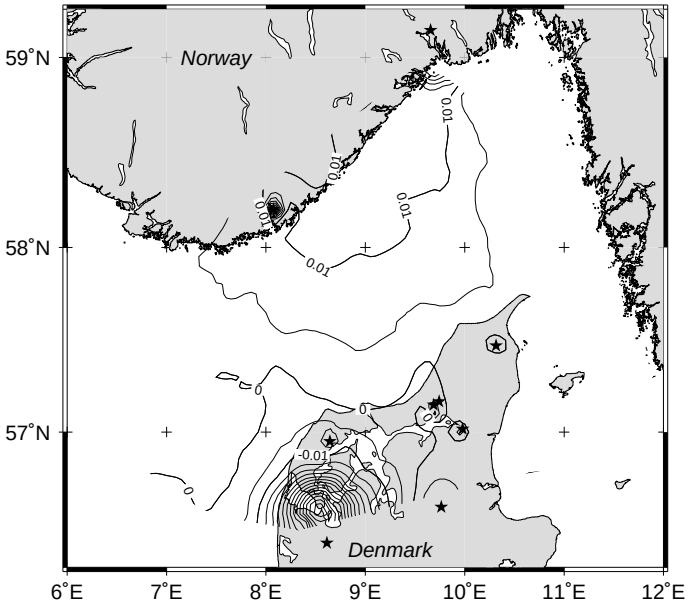

Figure 13: Contribution of 9 points of UEGN94 network (shown by asterisks) into geoid SMA2 at 3271 points of geoid grid ($3' \times 3'$); contour interval: 0.005 m

Statistics of differences dN (3271 points)	Minimum	Maximum	Mean	rms	Standard deviation
Differences: sol. SMA2−sol. SMA1	-0.0781	0.0477	0.0025	0.0103	0.0100

Table 11: Contribution [m] of 9 points of the UEGN94 network to the geoid solutions SMA2

These solutions were chosen as the most appropriate versions from various approximations (according to Section 7.3) either by means of radial multipole potentials of one degree only or by means of a combination of them with different degrees. The second approach provides on the whole a more stable process of the approximation with a smaller number of such potentials. As a result, for data Set 1 and Set 2 it was sufficient to create models consisting of 382 radial multipole potentials only. Statistics of comparison are shown in Table 10, and reflects a good agreement with the solutions of collocation and collocation with regularization (see Table 7). Table 11 illustrates the contribution of 9 points of the UEGN94 network into the geoid solutions SMA2. In spite of practically the same qualitative picture of Fig. 13 in comparison with Fig. 10 and Fig. 11, here the contribution is smaller (Table 11 vs. Table 9). The latter is also valid for the other solutions, which were omitted here.

Finally we should note the computational aspect of these two approaches. In the case of collocation or collocation with regularization methods the basic matrix with the dimensions 3370×3370 (for Set 1) or 3379×3379 (for Set 2) has to be inverted. In the case of a direct approximation by radial multipole potentials we have to invert

(on the re-adjustment step) the matrix with the dimension 382 × 382 only. Thus, practically the same or even better results can be obtained much faster. In other words, the last approach can be recommended especially for fast computations of the airborne geoid without loss of accuracy. Because the number of radial multipoles is only 10–20% of the total number of geodetic measurements the matrix inversion will be 25 – 100 times faster.

9 Combined solutions based on airborne/marine and airborne/marine/UEGN94 gravity data

In this section several geoid solutions were constructed on the basis of combined sets of airborne, marine and UEGN94 gravity anomalies. The computations are carried out for the same grid points ($3' \times 3'$) using the same approaches discussed in Section 8. Therefore point marine anomalies (mean accuracy $\approx$ 4.5 mGal) were added to Set1 and Set2 and the following initial data sets were generated for further data processing:

- Set 3 - 6886 airborne/marine gravity anomalies (mean accuracy $\approx$ 3.6 mGal), including Set1;
- Set 4 - 6895 gravity anomalies, including Set3 and supplemented by 9 points of UEGN94 absolute gravimetric network (mean accuracy $\approx$ 0.014 mGal), which are surrounding the Skagerrak area.

Fig. 14 illustrates the distribution of the initial airborne/marine/UEGN94 gravity anomalies according to Set3 and Set4. The results of the application of the "remove-restore" procedure to each data set ($\delta\Delta g = \Delta g - \Delta g_{\mathrm{EGM96}}$) can be found in Table 12.

After the prediction of the values $\delta\Delta g$ and δN, the geoid undulations were restored as $N = \delta N + N_{\mathrm{EGM96}}$ without terrain corrections. The essential parameters (Table 13) of the ECF were computed on the basis of the residual gravity anomalies $\delta\Delta g$ (Table 12).

Statistics (6886 points)	Minimum	Maximum	Mean	rms	Standard deviation
Initial airborne/marine Δg: set of 6886 points	-52.7	49.6	-4.4	14.5	13.8
$\delta\Delta g = (\Delta g - \Delta g_{\mathrm{EGM96}})$	-45.9	53.8	-2.7	10.3	9.9

Table 12: Statistics of the point Δg and residual $\delta\Delta g$ airborne/marine gravity anomalies [mGal]

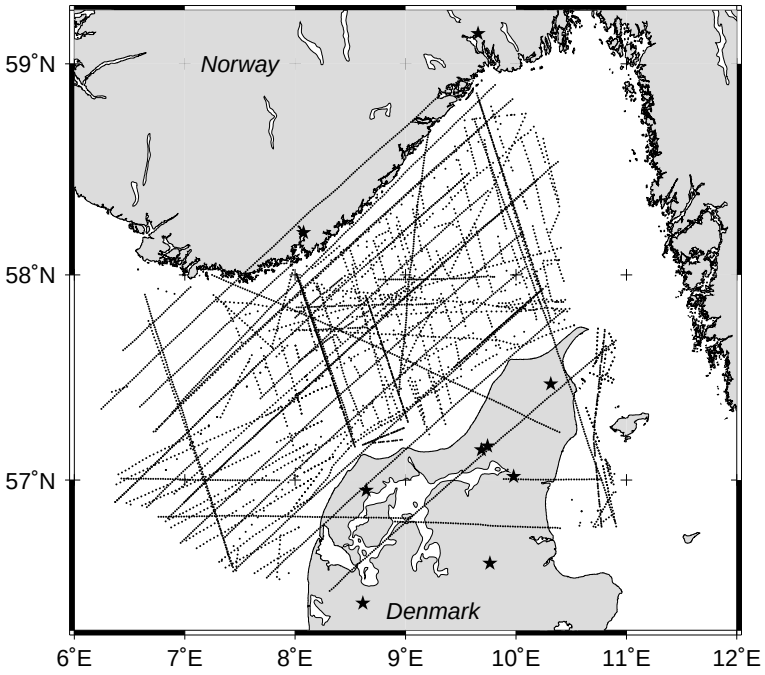

Figure 14: Distribution of initial airborne/marine gravity anomalies Δg (6886 point values) in the Skagerrak area (9 points of UEGN94 gravimetric network are shown by asterisks)

Region	Variance [mGal^2]	Correlation length [degree]	Parameter of Curvature
Skagerrak	98.7424	0.119889	3.9816

Table 13: Essential parameters of empirical covariance function, constructed for airborne and marine gravity anomalies

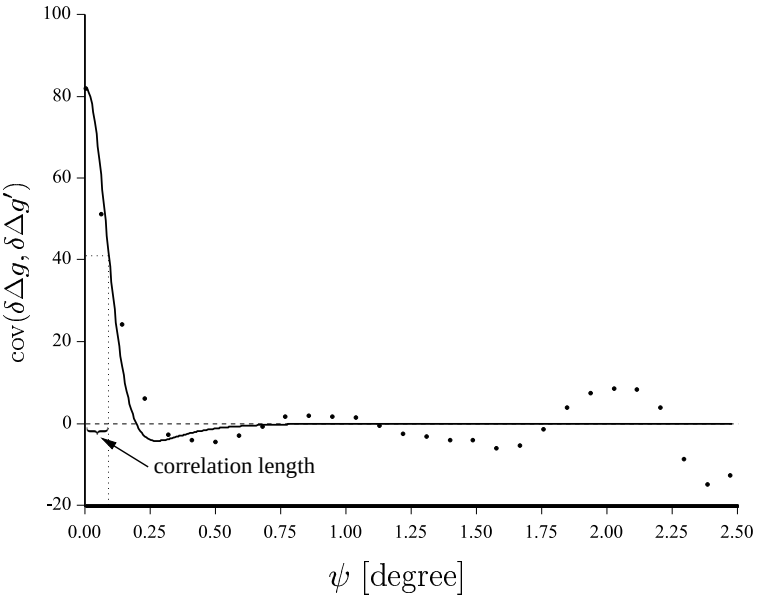

Figure 15: Empirical (dotted) and analytical (solid) covariance functions [mGal^2], based on 6886 airborne/marine $\delta\Delta g = (\Delta g - \Delta g_{\mathrm{EGM96}})$; analytical function represented by ***dipole*** kernel

ACF	Degree m	Scale-factor c in Eq. (44)	Bjerhammar sphere radius [meters]	Relative accuracy of ECF-fit [%]	Correlation length [degree]	Parameter of Curvature
Dipole kernel	1	$1.8135 \cdot 10^{-20}$	6344996.17	11.2	0.122362	3.2848
Quadrupole kernel	2	$1.5854 \cdot 10^{-22}$	6340467.24	12.3	0.122405	3.1537

Table 14: Parameters of the analytical covariance functions, constructed for airborne and marine gravity anomalies

---

In view of ECF fitting, the following ACFs turned out to be sufficient for further practical application: ***Dipole kernel*** (Table 14, Fig. 15), which corresponds to ***Poisson*** kernel without harmonics of degree zero, and ***Quadrupole kernel*** (Table 14) or a special combination of ***Krarup/Poisson*** kernels without harmonics of degree zero and degree one. Again, because of the slightly better fit of the dipole kernel, this one was selected for the following solutions.

To illustrate the geoid prediction by collocation and collocation with regularization techniques we again introduce the corresponding abbreviations:

- ASC1: Collocation solution for Airborne/marine geoid, based on Set3
- ASC2: Collocation solution for airborne/marine/UEGN94 geoid, based on Set4 (Fig. 16)
- ASR1: Collocation with regularization solution for airborne/marine geoid, based on Set3
- ASR2: Collocation with regularization solution for airborne/marine/UEGN94 geoid, based on Set4 (Fig. 17)

Fig. 18 and Fig. 19 illustrate the comparison of ASC2 and ASR2 solutions with the Nordic countries geoid (Forsberg, 2000). Table 16 and Table 17 reflect this independent comparison and allow to make the following conclusions:

1. Including only 9 points of UEGN94 leads to a better agreement of the regularization solution ASR2 with Forsberg's geoid, in terms of the mean difference,
2. The regularization solutions ASR1 and ASR2 provide smaller rms geoid differences than the collocation solutions ASC1 and ASC2.
3. In the case of the combined solutions ASR1 and ASR2 we got a smaller regularization parameter ($\alpha \approx 3$) than for airborne-only solutions ($\alpha \approx 5$) because of the denser coverage with observed data.

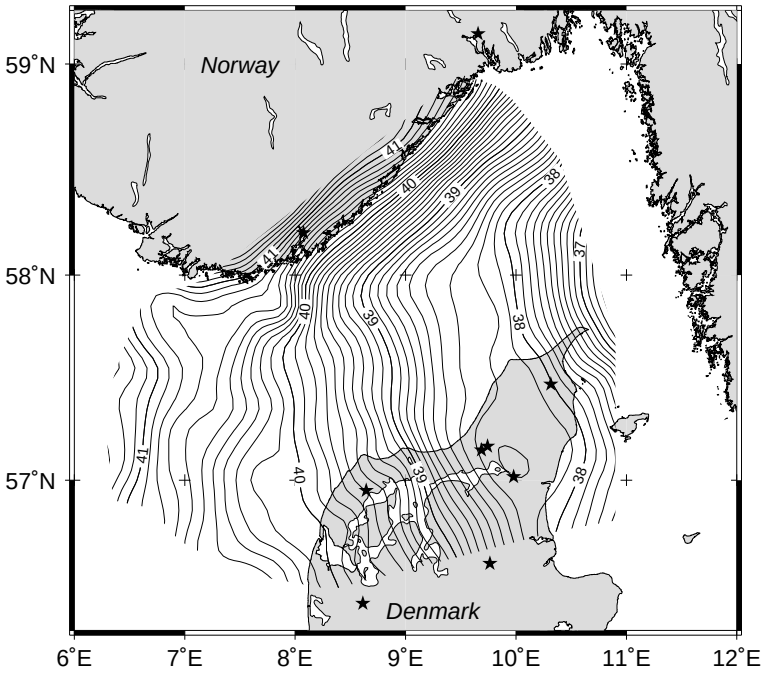

Figure 16: Airborne/ marine/UEGN94 geoid solution ASC2, based on the collocation method with dipole kernel; contour interval: 0.1 m; 9 points of UEGN94 network are shown by asterisks

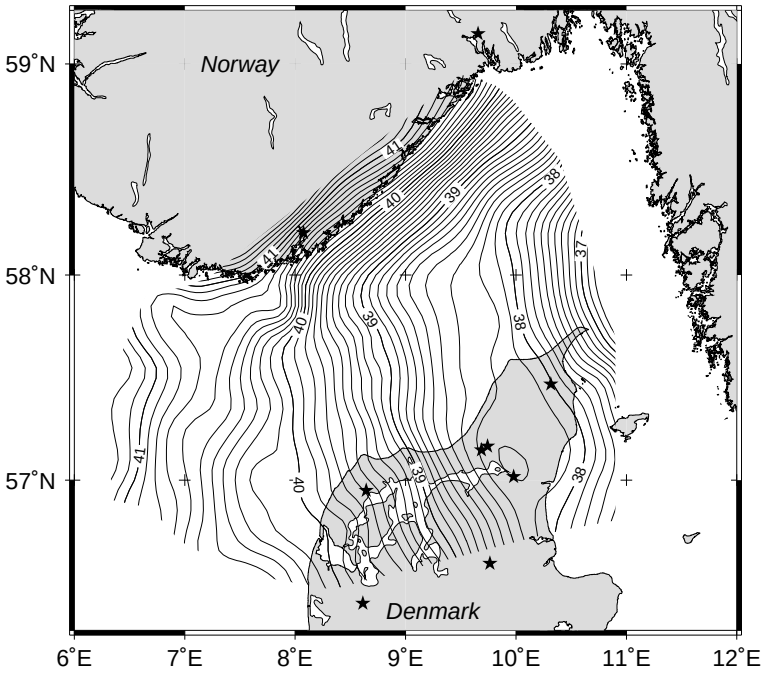

Figure 17: Airborne/ marine/UEGN94 geoid solution ASR2, based on the regularization method with dipole kernel; contour interval: 0.1 m; 9 points of UEGN94 network are shown by asterisks

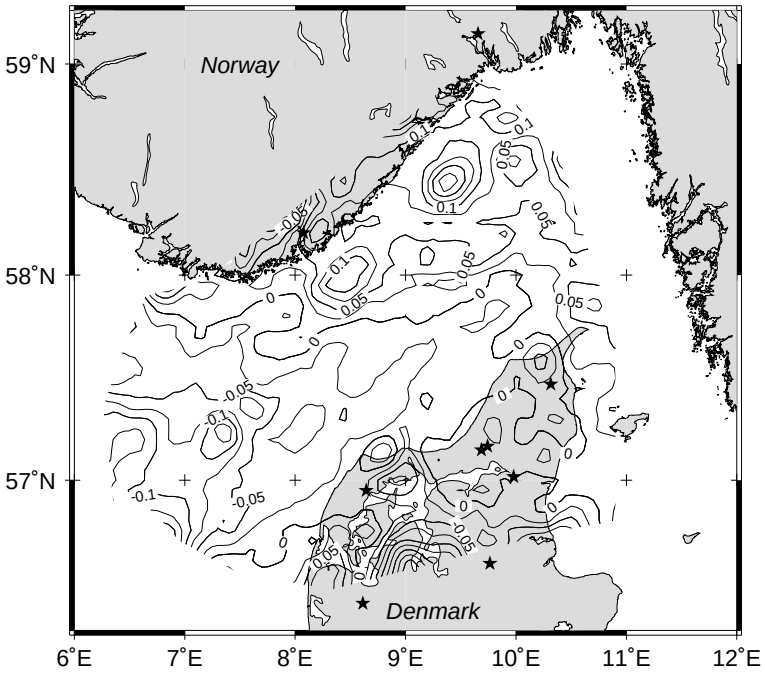

Figure 18: Differences between ASC2 geoid, based on the collocation method with dipole kernel, and Forsberg's geoid; contour interval: 0.025 m); 9 points of UEGN94 network are shown by asterisks

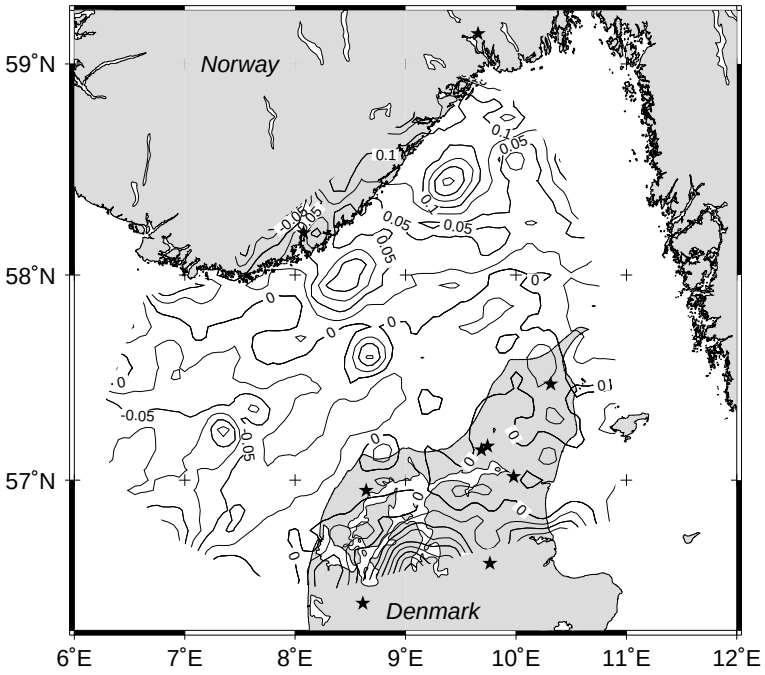

Figure 19: Differences between ASR2 geoid, based on the regularization method with dipole kernel, and Forsberg's geoid; contour interval: 0.025 m; 9 points of UEGN94 network are shown by asterisks

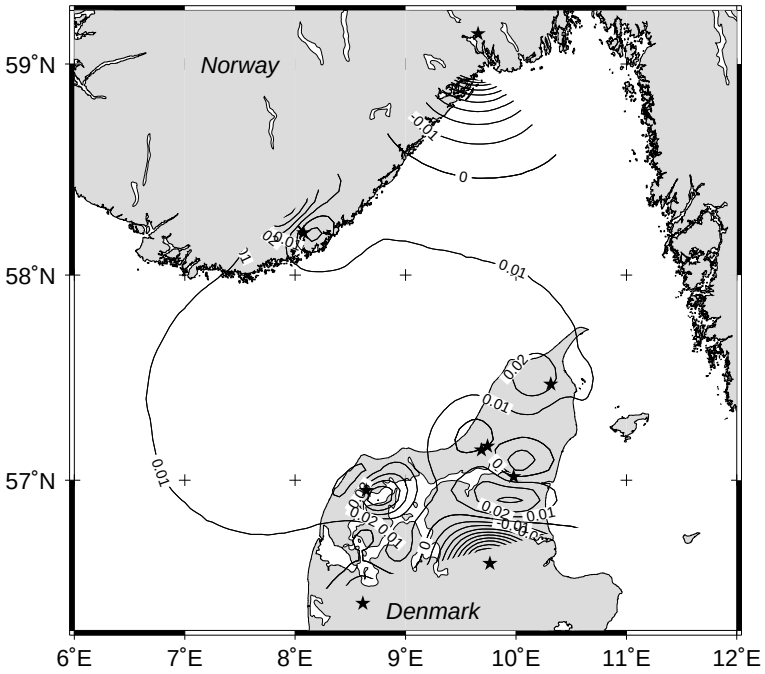

Figure 20: Contribution of 9 points of UEGN94 network (asterisks) to geoid ASC1: differences of solutions ASC2 minus ASC1; contour interval: 0.01 m

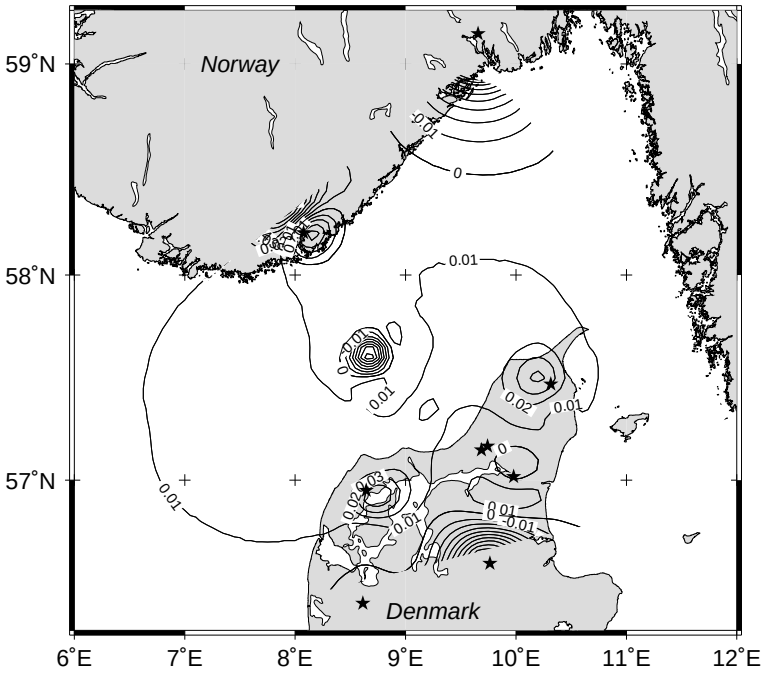

Figure 21: Contribution of 9 points of UEGN94 network (asterisks) to geoid ASR1: differences of solutions ASR2 minus ASR1; contour interval: 0.01 m

Statistics	Minimum	Maximum	Mean	rms	Standard deviation
Collocation method: Solution ASC2					
Predicted geoid undulations N	36.7087	41.6511	39.3901	39.4071	1.1566
Regularization method: Solution ASR2					
Predicted geoid undulations N	36.7401	41.6460	39.3873	39.4042	1.1522
Differences between two solutions					
ASR1 – ASC1	-0.0565	0.0435	-0.0019	0.0116	0.0114
ASR2 – ASC2	-0.0888	0.0327	-0.0028	0.0126	0.0123

Table 15: Statistics for final versions of airborne/marine/UEGN94 geoids [m], computed at 3271 points of geoid grid ($3' \times 3'$)

Statistics of differences δg (3271 points)	Minimum	Maximum	Mean	rms	Standard deviation
Collocation method: Solution ASC1 ($\alpha = 1$)					
dN = Forsberg's grid values N – predicted N	-0.1984	0.1993	0.0105	0.0554	0.0544
Regularization method: Solution ASR1 ($\alpha = 2.9877$)					
dN = Forsberg's grid values N – predicted N	-0.1920	0.1828	0.0123	0.0495	0.0479

Table 16: Differences dN between Forsberg's geoid grid ($3' \times 3'$) and their predicted values [m] based on 6895 gravity anomalies

---

In the following, airborne/marine/UEGN94 geoids were constructed using radial multipole potentials to represent the anomalous potential T. In contrast to the approximation of airborne data only (see Section 8) in this case some additional difficulties arose, since a solution of the special non-linear inverse problem (Section 7.3) requires to determine the locations of the eccentric multipoles from a preliminary analysis of the initial gravity data. The direct creation of the empirical function (EIF) leads to unstable results if the initial data are located at different levels (for instance, airborne and marine heights).

Statistics of differences dN (3271 points)	Minimum	Maximum	Mean	rms	Standard deviation
Collocation method: Solution ASC2 ($\alpha = 1$)					
dN = Forsberg's grid values $N-$ predicted N	-0.2046	0.2042	0.0024	0.0574	0.0573
Regularization method: Solution ASR2 ($\alpha = 2.9877$)					
dN = Forsberg's grid values $N-$ predicted N	-0.1946	0.1857	0.0053	0.0512	0.0509

Table 17: Differences dN between Forsberg's geoid grid ($3' \times 3'$) and predicted values [m] based on 6895 gravity anomalies, including 9 points of UEGN94 network

Statistics	Minimum	Maximum	rms
Collocation method: Solution ASC1	0.050	0.136	0.062
Regularization method: Solution ASR1	0.051	0.136	0.064
Collocation method: Solution ASC2	0.049	0.133	0.061
Regularization method: Solution ASR2	0.050	0.135	0.063

Table 18: Accuracy estimation of the predicted geoid heights [m]

Statistics of differences dN (3271 points)	Minimum	Maximum	Mean	rms	Standard deviation
Collocation method					
Differences: sol. ASC2−sol. ASC1	-0.1084	0.0601	0.0080	0.0147	0.0123
Regularization method					
Differences: sol. ASR2−sol. ASR1	-0.1082	0.0796	0.0071	0.0151	0.0133

Table 19: Contribution [m] of 9 points of UEGN94 network into geoid solutions

Statistics of differences dN (3271 points)	Minimum	Maximum	Mean	rms	Standard deviation
Solution SMA3	-0.1826	0.1869	0.0179	0.0474	0.0438
Solution SMA4	-0.1573	0.1960	0.0191	0.0481	0.0442
Solution SMA5	-0.2824	0.2137	-0.0115	0.0607	0.0596
Solution SMA6	-0.2806	0.2099	-0.0056	0.0621	0.0618

Table 20: Differences dN [m] between Forsberg's geoid grid ($3' \times 3'$) and solutions based on radial multipole potentials

Statistics of differences dN (3271 points)	Minimum	Maximum	Mean	rms	Standard deviation
Differences: sol. SMA4−sol. SMA3	-0.0998	0.0073	-0.0011	0.0110	0.0110
Differences: sol. SMA6−sol. SMA5	-0.0866	0.0355	-0.0059	0.0131	0.0117

Table 21: Contribution [m] of 9 points of UEGN94 network into geoid solutions

---

To illustrate this situation we decided to build the following models. At first, *only a re-adjustment* of the multipole moments for solutions SMA1 and SMA2 was applied without the determination of the locations of the multipoles (SMA). In this way the following models have been created:

- SMA3: SMA solution for airborne/marine geoid (with application of multipoles from 1 up to 8 degrees), based on Set3 (382 multipoles);
- SMA4: SMA solution for airborne/marine geoid (with application of multipoles from 1 up to 8 degrees), based on Set4 (382 multipoles).

Secondly, the Sequential Multipole Analysis was applied and after final re-adjustment we got two more SMA models:

- SMA5: SMA solution for airborne/marine geoid (with application of multipoles from 0 up to 8 degrees), based on Set3 (490 multipoles);
- SMA6: SMA solution for airborne/marine/UEGN94 geoid (with application of multipoles from 0 up to 8 degrees), based on Set4 (490 multipoles).

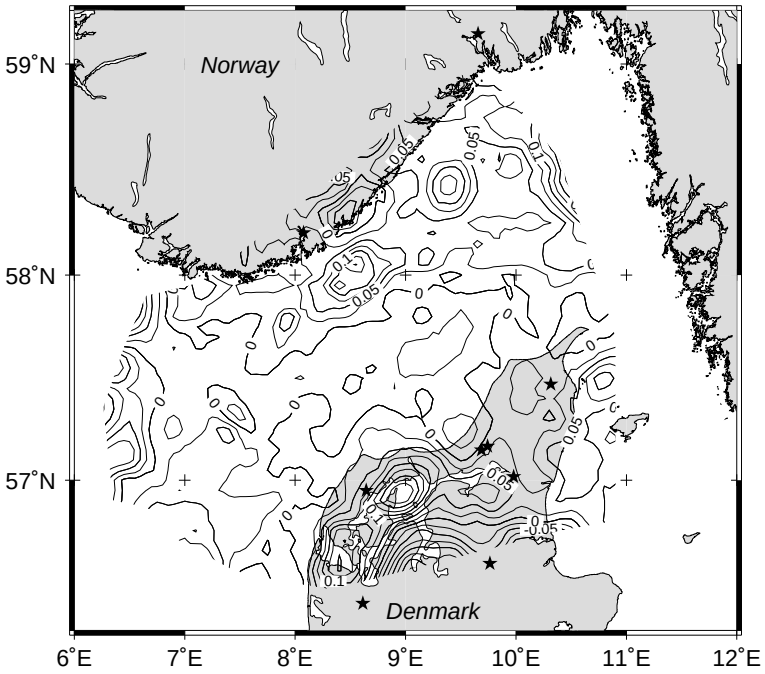

Figure 22: Differences between geoid SMA4, based on the approximation by radial multipole potentials, and Forsberg's geoid; contour interval: 0.025 m

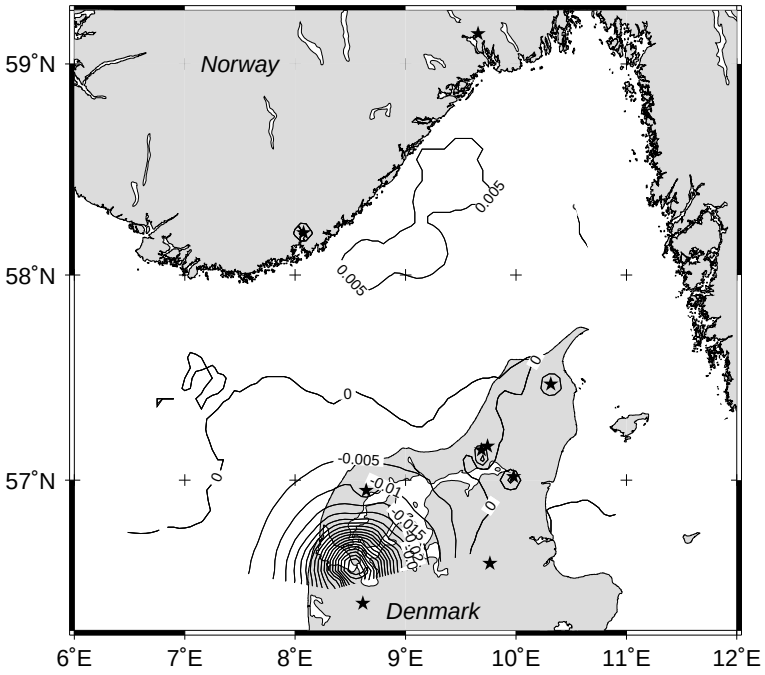

Figure 23: Contribution of 9 points of UEGN94 network (asterisks) to geoid SMA3: differences of solutions SMA4 minus SMA3; contour interval: 0.005 m

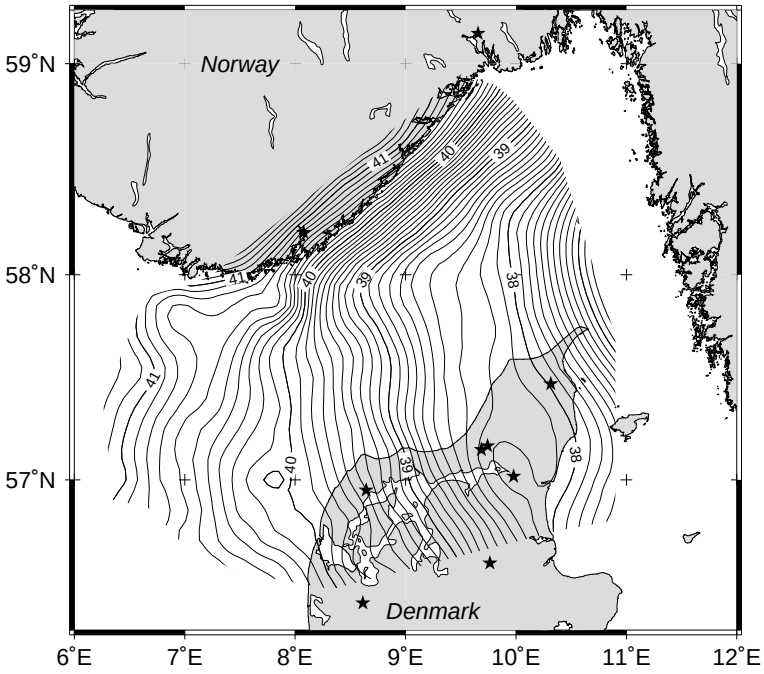

Figure 24: Airborne/ marine/UEGN94 geoid solution SMA4, based on the approximation by radial multipole potentials and computed at grid points ($3' \times 3'$); contour interval: 0.1 m; 9 points of UEGN94 network are shown by asterisks

To our own surprise, the solutions SMA3 and SMA4 are in better agreement (see Fig. 22, Table 20) with the Nordic countries geoid, although the SMA5 and SMA6 models include much more (490 instead of 382) multipoles of different degrees. A reduction of both airborne and marine data to a common reference level might have been necessary before applying the sequential multipole analysis method. This is left for further studies.

Among all solutions, these two multipole models (SMA3 and SMA4) are in best agreement with the solution of Forsberg (2000) (see Tables 6, 7, 10, 16, 17 and 20). Table 21 and Fig. 23 reflect the contribution of 9 points of UEGN94 network to the solution SMA4. Fig. 24 illustrates this airborne-marine-UEGN94 geoid SMA4, computed here by a simple re-adjustment of the "airborne" model SMA1, and represents a small but real practical improvement.

10 Conclusions

Finally an additional comparison between airborne/marine/UEGN94 and airborne or airborne/UEGN94 solutions was made and the corresponding statistics can be found in Table 22. Here, only geoid SMA2 was based on the direct approximation by radial multipole potentials with simple least squares adjustment by parameters which is characterized by a value of rms $\approx 4 - 5$ cm. The best agreement (rms = 1.6 cm) we get between the solutions ASR2 and AR2, which were based on collocation with regularization and additional information from the UEGN94 gravimetric network.

Statistics	Min.	Max.	Mean	rms	St. dev.
Differences with respect to regularization solution (ASR2)					
ASR2 – AC1 (airborne)	-0.131	0.133	0.007	0.027	0.026
ASR2 – AR1 (airborne)	-0.112	0.124	0.008	0.024	0.023
ASR2 – AC2 (airborne/UEGN94)	-0.066	0.107	0.000	0.019	0.019
ASR2 – AR2 (airborne/UEGN94)	-0.055	0.104	0.001	0.016	0.016
ASR2 – SMA2 (airborne/UEGN94)	-0.166	0.194	0.014	0.042	0.040
Differences with respect to collocation solution (ASC2)					
ASC2 – AC1 (airborne)	-0.116	0.123	0.010	0.028	0.026
ASC2 – AR1 (airborne)	-0.104	0.136	0.010	0.032	0.030
ASC2 – AC2 (airborne/UEGN94)	-0.074	0.096	0.002	0.019	0.019
ASC2 – AR2 (airborne/UEGN94)	-0.069	0.122	0.003	0.024	0.024
ASC2 – SMA2 (airborne/UEGN94)	-0.176	0.258	0.017	0.050	0.047

Table 22: Statistics of differences between airborne/marine/UEGN94 and airborne or airborne/UEGN94 geoids [m], computed at 3271 grid points ($3' \times 3'$)

In summary we can conclude:

- Collocation with regularization provides a slightly better accordance in terms of rms with Forsberg's geoid than standard collocation with the same reproducing kernel.
- Including additional information from 9 points of the UEGN94 absolute gravity network leads to an almost perfect agreement in the mean level of the solutions derived here compared to Forsberg's geoid covering the Nordic countries.
- For this reason, collocation with regularization based on Eq. (46) can be recommended for stable computations of airborne geoids, with the use of additional absolute gravimetric data to get the reference level (an ideal situation would be the inclusion of GPS-leveling).
- The approximation by radial multipole potentials can be recommended especially for fast computations of airborne geoids without degradation of accuracy with respect to collocation.

The independent comparison of the geoids derived here with the geoid solution for the Nordic countries agrees on a level of 5 cm. This value corresponds to the estimation of "relative geoid accuracies below 10 cm" in the Skagerrak area according to Forsberg et al. (2000).

Note finally, that both in case of the model approach and in case of the collocation/regularization method only singular point harmonic functions have been applied.

References

Abrikosov, O.A. (2000) On the determination of the regularization parameter in least squares collocation. Geodynamics, No. 2, Lviv

Aleksidze, M.A. (1966) On the representation of the anomalous gravity field. Dokl. akad. nauk. SSSR, Tom 170, No. 4, (in Russian)

Barthelmes, F. (1982) Representation of the Geopotential by Buried Point Masses Using an Algorithm to Find the Magnitudes and Plausible Positions of the Masses. Nabljudenija iskusstvennych sputnikov Zemli, No. 20, 1980, 491–501, Sofia

Barthelmes, F. (1984) Optimal approximation of the geopotential by a minimal number of point masses. Nabljudenija iskusstvennych sputnikov Zemli, No. 21, 1982, 124–130, Moscow, (in Russian)

Barthelmes, F. (1986) Untersuchungen zur Approximation des äußeren Schwerefeldes der Erde durch Punktmassen mit optimierten Positionen. Veröff. Zentralinst. Physik der Erde Nr. 92, Potsdam

Barthelmes, F. (1988) Local gravity field approximation by point masses with optimized positions. In: Proceedings of the 6th International Symposium "Geodesy and Physics of the Earth", Part 2, Gravity field variations, 157–167, Veröff. Zentralinst. Physik der Erde Nr. 102, Potsdam 1989

Barthelmes, F., Kautzleben, H. (1983): A New Method of Modeling the Gravity Field of the Earth by Point Masses. Proc. of the IAG Symposia, 1, 442-448, Dep. of Geodetic Science and Surveying, The Ohio State University

Darwin, G. (1884) On the figure of equilibrium of a planet of heterogeneous density. Proceeding of the Royal Society, 36, 158–166

Forsberg, R. (2000) Private communication.

Forsberg, R., Tscherning, C.C. (1981) The use of height data in gravity field approximation by collocation. J. Geophys. Res., 86, No. B9, 7843–7854

Forsberg, R., Solheim, D., Kaminskis, J. (1997) Geoid of the Nordic and Baltic area from gravimetry and satellite altimetry. In: Segawa, J., Fujimoto, H., Okubo, S., eds.: Gravity, Geoid and Marine Geodesy, 540–547. Springer-Verlag, New York

Forsberg, R., Hehl, K., Bastos, L., Gidskehaug, A., Meyer, U. (1997) Development of a geoid mapping system for coastal oceanography (AGMASCO). In: Segawa, J., Fujimoto, H., Okubo, S., eds.: Gravity, Geoid and Marine Geodesy, 163–170, Springer Verlag, New York

Forsberg, R., Olesen, A., Bastos, L., Gidskehaug, A., Meyer, U., Timmen, L. (2000) Airborne geoid determination. Earth, Planets and Space (spec. issue: proc. GPS-99 conference, Tsukuba, Japan, Oct. 1999) 52, 863–866

Gruber, T. (2000) Hochauflösende Schwerefeldbestimmung aus Kombination von terrestrischen Messungen und Satellitendaten über Kugelfunktionen. Scientific Technical Report, STR 00/16, GFZ Potsdam

Hauck, H., Lelgemann, D. (1984) Regional Gravity Field Approximation with Buried Masses Using Least-Norm Collocation. Manuscripta Geodaetica, 10, 50–58

Heiskanen, W.A., Moritz, H. (1967). Physical Geodesy, W.H. Freeman, San Francisco

Hobson, E.M. (1931) The Theory of Spherical and Ellipsoidal Harmonics. University Press, Cambridge

Kearsley, A.H.W., Forsberg, R., Olesen A., Bastos, L., Hehl, K., Meyer, U., Gidskehaug, A. (1998) Airborne gravimetry used in precise geoid computations. Journal of Geodesy 72, 600–605

Krarup, T. (1969) A Contribution to the Mathematical Foundation of Physical Geodesy. Danish Geod. Inst. Public., No. 44, Copenhagen

Lauritzen, S. (1973) The Probabilistic Background of some Statistical Methods in Physical Geodesy. Danish Geod. Inst. Public., No. 48, Copenhagen

Lemoine, F.G., Kenyon, S.C., Factor, J.K., Trimmer, R.G., Pavlis, N.K., Chinn, D.S., Cox, C.M., Klosko, S.M., Luthcke, S.B., Torrence, M.H., Wang, Y.M., Williamson, R.G., Pavlis, E.C., Rapp, R.H., Olson, T.R. (1998) The Development of the Joint NASA GSFC and the National IMagery and Mapping Agency (NIMA) Geopotential Model EGM96. NASA Technical Paper NASA/TP–1998–206861, Goddard Space Flight Center, Greenbelt, USA

Marchenko, A. (1987) Description of the Earth's gravity field by the system of potentials of non-central multipoles, I. Theoretical background; II. Preliminary multipole analysis. Kinematics and Physics of Celestial Bodies, Kiev, 3, No. 2, 54–62; 3, No. 3, 38–44, (in Russian).

Marchenko, A.N. (1998) Parameterization of the Earth's Gravity Field: Point and Line Singularities. Lviv Astronomical and Geodetic Society, Lviv

Marchenko, A.N., Abrikosov, O.A. (1995). Geoid in the West Ukraine Area Derived by Means of the Non-Central Multipole Analysis Technique. Proceed. of the International Symposium No. 113 "Gravity and Geoid", 624–629, Graz, Austria, Springer-Verlag Berlin Heidelberg

Marchenko, A.N., Lelgemann, D. (1998) A classification of reproducing kernels according to their functional and physical significance. IGeS Bulletin N 8, International Geoid Service, Milan, 49–52.

Meshcheryakov, G.A., Marchenko, A.N. (1980). Point Mass Models of the Geopotential. Studying of the Earth as a Planet by Methods of Astronomy, Geophysics and Geodesy, Kiev, 1982, 121–131, (in Russian)

Moritz, H. (1980) Advanced Physical Geodesy. Wichmann, Karlsruhe

Morozov, V.A. (1987) Regular Methods for Solving Ill-posed Problems. Nauka, Moscow, (in Russian).

Neyman, Yr. (1979) Variational method of Physical Geodesy. Nedra, Moscow, (in Russian)

Rapp, R., Nerem R. (1995) A Joint GSFC/DMA Project for Improving the Model of the Earth's Gravitational Field. Proceed. of the International Symposium No 113 "Gravity and Geoid", Graz, Austria, 1994, Springer-Verlag Berlin Heidelberg, 413–422.

Scales, L.E. (1985) Introduction to Non-Linear Optimization. Macmillan Computer science series, Macmillan London and Basingstoke

Tikhonov, A.N., Arsenin, V.Y. (1974). Methods of solution of ill-posed problems. Nauka, Moscow, (in Russian).

Tscherning, C.C. (1972) Representation of covariance function related to the anomalous potential of the Earth's using reproducing kernels. Danish Geod. Institute Internal Report, No. 3, Copenhagen.

Tscherning, C.C., Rapp, R. (1974) Closed covariance expressions for gravity anomalies, geoid undulations, and deflections of vertical implied by anomaly degree variance models. Dep. of Geod. Sci., Ohio State Univ., Rep. No. 208, Columbus.